Technical report; TR - 285

KNMI

Surface albedo derived from TOMS, GOME and MODIS and their application in NO_2 retrieval

H.T. van Dam

De Bilt, 2005

Koninklijk Nederlands Meteorologisch Instituut

Technical report = technisch rapport; TR 285

De Bilt, 2005

PO Box 201
3730 AE De Bilt
Wilhelminalaan 10
De Bilt
The Netherlands
http://www.knmi.nl
Telephone +31(0)30-220 69 11
Telefax +31(0)30-221 04 07

Author: Dam, H.T. van

Surface albedo derived from TOMS, GOME and MODIS and their application in NO_2 retrieval

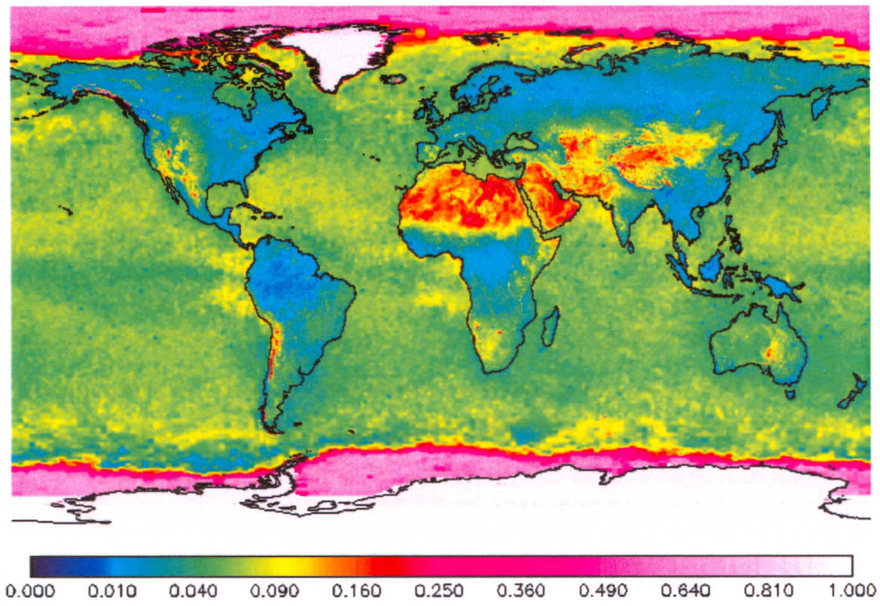

H.T. van Dam
July 2005

Supervisors: dr. R.J. van der A (KNMI, De Bilt)
dr. H.J. Eskes (KNMI, De Bilt)
prof. dr. H. Kelder (Eindhoven University of Technology; KNMI, De Bilt)

Eindhoven University of Technology
Department of Applied Physics

TU/e technische universiteit eindhoven

KNMI

1 Index

2 Introduction

Land surface albedo is one of the important parameters characterizing the earth's and atmosphere's energy balance. Albedo is related to land surface reflectance by directional integration and is therefore dependent on the bidirectional reflectance distribution function (BRDF), which describes how the reflectance depends on view and solar angles. Specification of the BRDF provides land surface reflectance explicitly in terms of its spectral, directional, spatial and temporal characteristics. Figure 2.1 illustrates key causes for land surface reflectance anisotropy and the resulting nonlinear relationship between albedo and the reflectance observed by a satellite from a given direction.

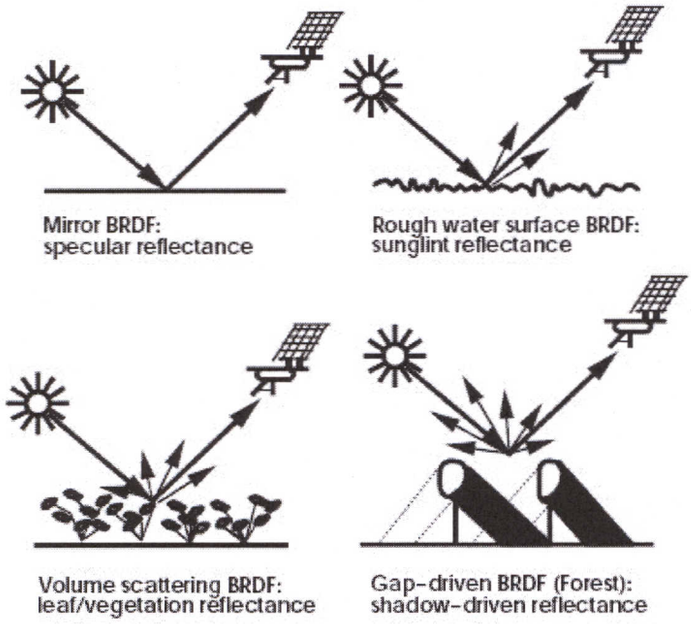

Fig 2.1: Basic reasons for land surface reflectance anisotropy:
upper left: specular reflectance; upper right: specular scattering such as sun glint, also observed where forward-scattering leaves or soil elements are present; down left: radiative transfer-type volumetric scattering by finite scatterers (leaves of plant canopies) that are uniformly distributed, potentially nonuniformly inclined and them-selves have anisotropic reflectance; down right: geometric-optical surface scattering, which is given by shadow-casting and mutual obscuration of three-dimensional surface elements, for example of trees in a sparse forest or brushland, or of clods on a ploughed field or of rock-strewn deserts. In natural systems, all types of scattering are likely to occur simultaneously.

Albedo quantifies the radiometric interface between land surface and atmosphere. On the one hand it defines the lower boundary for atmospheric radiative transfer, on the other hand it details the total shortwave energy input into the biosphere and it is a key factor in the surface energy balance.
The BRDF is also a potential source of biophysical information about the land surface viewed. Most importantly, however, it allows specification of land surface albedo.
Both BRDF and albedo are determined by land surface structure and optical properties. Surface structure influences the BRDF for example by shadow-casting, mutual view

shadowing, and the spatial distribution of vegetation elements. Surface optical characteristics determine the BRDF for example through vegetation-soil contrasts and the optical attributes of canopy elements. As a consequence, the spatial and temporal distribution of these land surface properties as seen in BRDF and albedo features reflect a variety of natural and human influences on the surface that are of interest to global change research. Such influences on albedo are for example due to agricultural practices, deforestation and urbanization; the phenological cycle, for example seasonal dependency and agricultural green-up/harvesting; meteorological parameters, for example soil wetness and snowfall distribution; and climatological trends, for example desertification, vegetation cover changes, and snowfall patterns.

Albedo is a fundamental parameter for climate modelling, since it is a property that drives much of the energy flux at the land boundary layer. Global maps of land surface albedo, which are provided at fine to coarse scales using the BRDF/Albedo Product, will be extremely useful to global and regional climate modelling.

Climate models currently employ albedo values derived from the land cover type of each grid box. The underlying albedo tables go back to various field measurements, coarse-resolution top-of-atmosphere observations or are computed from models. However, there is a need for a more accurate specification of albedo as a function of land cover type, season and solar zenith angle. This can only be achieved from accurate derivations of kilometre-scale albedo datasets for large areas, allowing the study of the magnitude distribution and of the spatial aggregation of values to coarser resolution for each land cover type and land cover mosaic. Remote sensing is the most suitable technique for deriving large consistent datasets of land surface parameters.

New remote sensing instruments like SCIAMACHY and OMI have a much higher resolution than the TOMS and GOME instruments, which are used for the determination of the current albedo dataset at the KNMI. Therefore the new MODIS albedo dataset, which is at a much higher resolution than the current albedo dataset, is investigated in this study. The goal of the study described in this report is to quantify and understand the differences between the surface albedo datasets.

Surface albedo is among other things used in the retrieval of NO_2, SO_2, CH_2O and ozone. As a boundary condition at the earth's surface, the albedo values have a large influence on the determined concentration values. NO_2 retrieval at the KNMI is performed with the SCIAMACHY instrument and the albedo dataset from TOMS and GOME, which is at a much coarser resolution, is used. Therefore is also investigated the effect of the new MODIS albedo dataset on the NO_2 retrieval. [9]

3 Definitions

3.1 Satellite geometry

Remote sensing satellite measurements are performed using a geometry as shown schematically in figure 3.1.

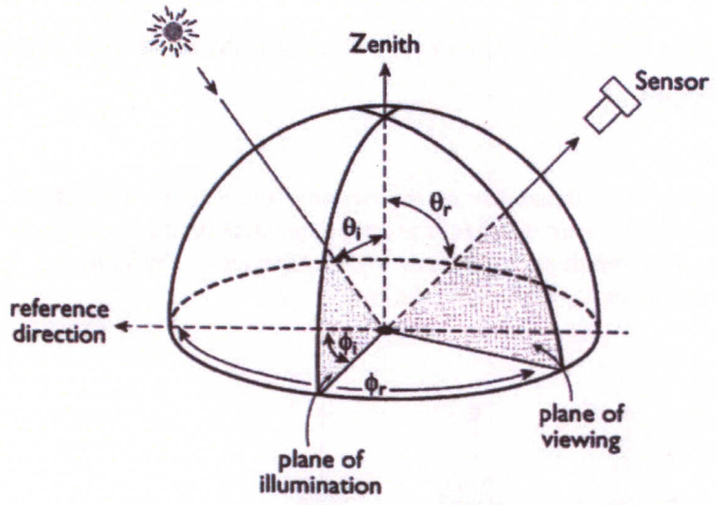

Figure 3.1: Schematic overview of the geometry of a satellite measurement.

Light with wavelength λ from the sun enters the atmosphere and reaches a piece of surface (pixel) at an solar angle θ_i with respect to the normal (zenith) in that particular pixel and an azimuth angle φ_i with respect to a reference direction. The measured light is the light which is reflected at an angle θ_r with respect to the normal and the light at an azimuth angle φ_r with respect to the reference direction.

3.2 Reflectance and BRDF

The amount of the light that reaches the satellite sensor is determined by the atmosphere composition and the earth surface properties, from which the latter is described by the bidirectional reflectance distribution function (BRDF). This describes how the reflectance depends on view and solar angles. It is defined as the ratio of the reflected radiance in a single view direction and the irradiance coming from some incident solar direction.
From the measured radiance at the top of atmosphere the reflectance R is determined with:

$$R(\lambda;\theta_r,\theta_i,\phi_r-\phi_i)=\frac{\pi\cdot I}{\mu_i E_i} \qquad (1)$$

in which I is the radiance at the top of atmosphere as measured by the satellite sensor. μ_i is defined as $\mu_i=|\cos\theta_i|$ and $\mu_i E_i$ is the solar irradiance at the top of atmosphere incident on the horizontal surface. Irradiance is the integral of the radiance weighted with μ over 2π steradians. [5],[6]

3.3 Albedo

Albedo is defined as the ratio of upwelling to downwelling radiative flux at the surface and thus only depends on the solar zenith angle and the wavelength. Mathematically albedo is defined as the integral of R over all viewing angles and azimuth angles:

$$A = \frac{1}{\pi} \int_0^{2\pi} \int_0^1 \mu R(\lambda; \theta_r, \theta_i, \phi_r - \phi_i) d\mu d\phi \qquad (2)$$

Here φ is the relative azimuth view angle and $\mu = |\cos\theta_r|$, in which θ_r is the zenith view angle. Albedo is also called reflectivity. [6]

3.4 Lambertian surface

If the radiance emitted by a surface is not dependent on the viewing zenith angle, the surface is called Lambertian. In that case the measured radiance is only dependent on the wavelength and the solar zenith angle. This solar zenith angle dependency is characterised in figure 3.2. It shows that the larger the solar zenith angle, the smaller the reflectance.

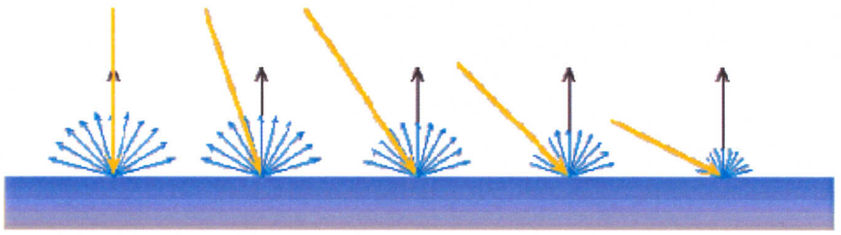

Figure 3.2: The solar zenith angle dependency characterised for a Lambertian surface. The larger the solar zenith angle, the smaller the reflectance

3.5 Atmospheric scattering

When light from the sun enters the atmosphere, it scatters in the atmosphere by Rayleigh, Mie and in lesser amount by non-selective scattering before it scatters at the surface.
Rayleigh scattering mainly consists of scattering from atmospheric gases. This occurs when the particles are smaller than the wavelengths of the radiation. This type of scattering is therefore wavelength dependent. The amount of scattering is inversely proportional to the 4^{th} power of the wavelength, so when the wavelength decreases, the amount of Rayleigh scattering increases.
Mie scattering is caused by dust, pollen, smoke, water droplets and other particles in the lower part of atmosphere. It occurs when the particles are larger than the wavelengths of radiation and it is also wavelength dependent.
Non-selective scattering occurs in the lower part of the atmosphere, when the particles are much larger than the incident radiation. This type of scattering is not wavelength dependent and is primarily caused by haze.

3.6 Scattered light detection

Solar light reaches the detector at many ways. An infinite amount of ways for multiple scattering is possible. A few of them are shown in figure 3.3.

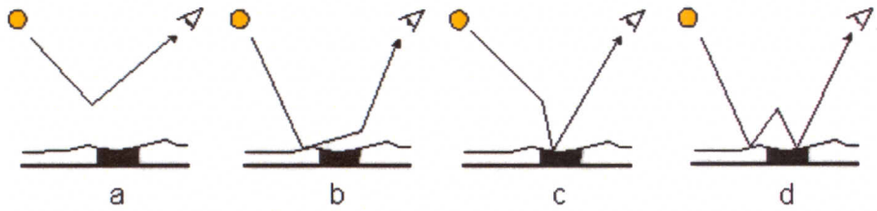

Figure 3.3: Several ways for solar light to reach the detector.

Solar light can for example scatter once (figure 3.3a) or several times in the atmosphere and then reach the satellite sensor. It can hit the surface at a point near the viewed surface pixel and reach the sensor by multiple scattering (figure 3.3b). It can reach the viewed surface pixel by multiple scattering and then go to the sensor (figure 3.3c). Another possibility is that the light scatters somewhere at the surface, scatters back in the atmosphere towards the selected pixel and then goes to the sensor (figure 3.3d). But about 80% of the light is directly scattered at the selected pixel at 440 nm, the wavelength of most interest in this report, because it is used in the NO_2 retrieval.

4 Satellite technical information

4.1 TOMS

Launched on 25 October 1978 from Vandenberg Air Force Base, California, the TOMS instrument aboard the NIMBUS-7 spacecraft was the first in a series of 4 TOMS instruments operated by the US National Oceanic and Atmospheric Administration (NOAA) and the US National Aeronautics and Space Administration (NASA). The succeeding TOMS instruments were flying aboard METEOR-3, ADEOS and EARTH PROBE. NIMBUS-7 was positioned in a sun-synchronous orbit at an altitude of 955 km and crosses the equator at about 11:15 local time in an ascending orbit. Its orbital period is 104.15 minutes, and consecutive equator crossings are separated by 26.1 degrees longitude. TOMS has a daily global coverage and a repeat cycle of 83 orbits. It scans in the cross-track direction in 3 degree steps from 51 degrees on one side of nadir to 51 degrees on the other. The field of view of 3x3 degrees results in a 50x50 km square at nadir. TOMS measures backscattered radiance at wavelength bands centred at 312.5, 317.5, 331.3, 339.9, 360.0 and 380.0 nm with a spectral resolution of 0.2 nm.

4.2 ERS-2 GOME

On April 21, 1995, the European Space Agency (ESA) launched the Global Ozone Monitoring Instrument aboard the second European Remote Sensing satellite (ERS-2). The satellite was flying in a sun-synchronous orbit and crosses the equator at 10:30 local time in a descending orbit at an altitude of 780 km. It has a scanning swath of 960 km, which is divided in 3 ground pixels. The scan measures 40 km in the direction of flight. The global coverage is 3 days with an orbital period of about 100 minutes. It measures with a spectral resolution of 0.2 nm in 5 spectral channels: 237-307, 307-315, 312-406, 397-609 and 576-794 nm.

4.3 TERRA MODIS

On 18 December 1999 the satellite TERRA was launched with the MODIS (MODerate resolution Imaging Spectroradiometer) instrument on board. This satellite crosses the equator at 10:30 in an ascending orbit at an altitude of 705 km. The MODIS instrument measures spectral bands in the range of 459 nm – 2155 nm with a spatial resolution at nadir of 500 m. Its field of view is 110° and it has a global coverage of 1-2 times per day with a repeat cycle of 16 days.

4.4 ENVISAT SCIAMACHY

SCIAMACHY, launched on March 1, 2002, onboard the ENVISAT satellite, covers the wavelength range 240-2380 nm with a spectral resolution between 0.2 and 1.5 nm. The ground pixel size varies between 30x60 km and 30x240 km. The satellite crosses the equator at 10:00 local time at an altitude of 800 km in a sun-synchronous descending orbit with a global coverage of 6 days.

5 NO_2 retrieval

Air pollution has become a global issue. Much of the anthropogenic air pollution travels long distances towards areas far from the emission source. Air pollution is composed of many environmental factors. They include carbon monoxide, nitrates, sulphur dioxide, ozone, lead and aerosols. Aerosols are composed of solid and liquid particles within the air and vary considerably in size, composition and origin. NO_2 is one of the most important air pollutants and it is an air pollution precursor.
The main source of NO_2 is emission from traffic, but heavy industry, fossil fuel power plants, biomass burning, lightning and volcanic eruptions are also important NO_2 emission sources. Its main effects are the following:

- It causes lung irritation and it aggravates cardiovascular and respiratory diseases.
- It affects plant life by premature leaf loss and inhibition of growth.
- It stimulates paint decolouration.
- It contributes to ozone and smog formation in the troposphere.

NO_2 measurements are performed using a spectrometer aboard a satellite, which is the SCIAMACHY instrument in this report. The reflected solar light is measured. Because every gas absorbs a different set of wavelengths, the atmosphere composition is determined by comparing the known and measured spectra, using the Differential Optical Absorption Spectroscopy (DOAS) technique. The measured spectra are used to retrieve slant column densities. These slant column densities are converted to vertical column densities using an air mass factor. This air mass factor is computed using a radiative transfer model and depends among others on the surface albedo. Tropospheric NO_2 values are expressed in vertical columns and have as unit molecules per cm^2.
The surface albedo is inversely proportional to the air mass factor and therefore it directly influences the sensitivity of the retrieval for boundary layer NO_2. High quality albedo maps in the relevant spectral range (around 440 nm) are essential for an accurate retrieval. [1]

6 Surface albedo determination

6.1 Lambertian Equivalent Reflectivity as determined by GOME

For GOME the Lambertian equivalent reflectivity is determined with the procedure as used by *Koelemeijer et al.*. This procedure is described here.
The reflectance at the top of atmosphere as measured by GOME is defined by equation 1. The measured reflectance can be considered as a mixed term of reflection at the atmosphere and of reflection at the surface.
An atmosphere is considered with an underlying surface and multiple reflections between the atmosphere and the surface are taken into account, but no multiple scattering in the atmosphere. Assumed is a multilayered Rayleigh-scattering atmosphere, bounded below by a Lambertian surface with an albedo A_s. Absorption by ozone is taken into account and the surface pressure was varied to take into account effects of the Earth's topography.
The reflectance for the combined atmosphere and surface system is the summation of all the light beams emergent at the top of atmosphere, as shown below in figure 6.1.

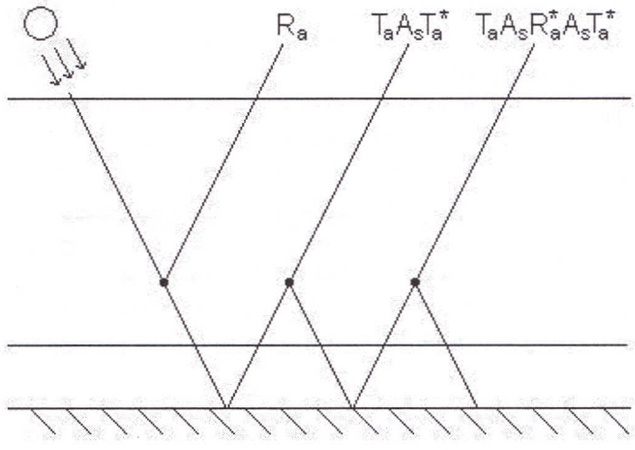

Figure 6.1: Contribution of the bidirectional reflectance from the atmosphere-surface system.

To describe the dependency of the measured reflectance R on the surface albedo A_s all surface reflection terms are added in a series, which results in equation 3:

$$R(\mu,\mu_0,\phi-\phi_0) = R_a(\mu,\mu_0,\phi-\phi_0) + \frac{A_s T(\mu_0) T^*(\mu)}{1 - A_s R_a^*} \qquad (3)$$

R_a denotes the reflectance from the atmosphere only. The second term represents the surface contribution. In this equation R_a^* is the reflectance of the atmosphere for the radiation from below. The term $T(\mu_0)$ is the total transmission function (direct plus diffuse) from the sun to the surface, while $T^*(\mu)$ is the total transmission function from the surface to the satellite.
The radiative transfer model DAK is used to create a lookup table of R_a, $T^*(\mu)$, $T(\mu_0)$ and R_a^* as a function of surface pressure, ozone column density and wavelength.
The Lambertian equivalent reflectivity (LER) $R_L(\lambda)$ is found for each pixel as the value of the effective surface albedo needed to match the measured reflectance at the top of atmosphere. Because of the assumption that the surface is Lambertian, the effective surface albedo value is equal to the effective surface reflectance value.

All $R_L(\lambda)$ spectra are sorted into grid cells of 1° x 1° and per month. For each grid cell the minimum value of R_L per month is searched at 670 nm out of all the 14.5 years of available data. At that wavelength the contrast between cloudy and cloud free pixels is large for most surface types and therefore clouds are filtered out better. For all the other wavelengths the corresponding value from the same measurement is stored in a database. [5]

6.2 Surface albedo as determined by TOMS

6.2.1 Lambertian equivalent reflectivity

For TOMS the Lambertian equivalent reflectivity is determined with the procedure as used by *Herman et al.*. This procedure is in many ways very similar to the GOME procedure and described here.

Assume an atmosphere, consisting of Rayleigh scatterers bounded by a surface whose Lambertian equivalent reflectivity $R_L(\lambda)$ is estimated from the measured radiances. The LER is the diffuse reflectivity that would need to be at the bottom of the atmosphere to explain the radiance that TOMS measures at the top of the atmosphere. For a pure Rayleigh atmosphere, $R_L(\lambda)$ is an estimate of the value of the BRDF of the surface at a given measurement geometry. If the true BRDF is anisotropic, $R_L(\lambda)$ will differ from the BRDF value, because of the mixing of reflection angles due to subsequent atmospheric scattering.

In the presence of clouds and aerosols, $R_L(\lambda)$ is greater than the BRDF of the surface, except when enough UV-absorbing aerosols are present to make the losses due to absorption greater than increases from backscattering.

It is possible to get a reflectivity higher than 100% under certain conditions such as sun glint. It is also possible to get a reflectivity less than zero if there is light absorbing dust in the atmosphere. This is because the reference is the scattering that is expected from a clear atmosphere.

TOMS measured both radiance and solar irradiance (using a diffuser plate) with the same instrument in order to determine initial radiance-irradiance ratios. For the remainder of the TOMS mission it was assumed that the solar irradiance remained constant for the 340-380 nm wavelength range.

In general, $R_L(\lambda)$ is affected by the presence of clouds, haze, and aerosols in each instrumental field-of-view unless the scene is clear. Even for the clearest of midday scenes, the earth surface is frequently covered by a thin, low lying surface haze whose scattering can slightly increase $R_L(\lambda)$ and also make the apparent BRDF, measured from space, slightly more isotropic by diffusing the reflected light. Because minimum $R_L(\lambda)$ values are used in this study, contamination by ground haze should be minimized and should closely represent the LER of the earth's surface.

Minimum reflectivities, in the processed 1 x 1.25 gridded LER values obtained from 14.5 years of data, were determined for each month of the year as well as over the entire data record. The resulting dataset has a majority of values tightly clustered about $R_L(\lambda)$ values of a few percent and a small set of statistically improbable outlier points. Outlier points caused by noise in the system or unusual atmospheric conditions were removed.

To find the minimum reflectivities for each 1x1.25 degrees pixel, the following procedure is used. Approximately 400 values for each pixel were assembled into monthly histograms after rejecting the infrequently found small negative values. The smallest $R_L(\lambda)$ values found for each pixel usually differ by at most 2%. In such cases, if the frequency of occurrence of the smallest value is at least half that of the second-smallest value, the smallest value is used. If the two smallest values are separated by less than 2%, but the frequency of occurrence of the smallest is less than half that of the second smallest, then the frequency-weighted average of these two values is used. If the separation between the smallest and second-smallest values is

at least 2%, then the smallest is used only if its frequency of occurrence exceeds ¾ that of the second smallest. In those few cases where this condition was not met (mostly at very high latitudes), the value at a particular pixel was obtained by distance-weighted interpolation with the 5-pixel by 5-pixel neighbourhood of the pixel in question. The above procedure results in the selection of the measured minimum value whenever its frequency of occurrence indicates that it is representative of the pixel and not an artefact of the LER determination. It also results in rejection of outlier values that are not statistically representative of the pixel. Aerosol contamination is also eliminated in this way, which results in slightly higher values than for GOME. [4]

6.2.2 Cloud fraction determination

The reflectivities include a modification for partial cloud coverage whenever the reflectivity is greater than 0.08. Because of this, larger values of the reflectivities do not represent ground LERs, but rather a weighted average of ground and cloud reflectivity that gradually deviates from the surface LER as the reflectivity increases. This does not affect the present calculations, since most of the cloud-free surface reflectivities in the wavelength range from 340-380 nm are less than 0.08.
Reflectivity is determined from the measurements at 360 nm. For a given TOMS measurement, the first step is to determine calculated radiances at 360 nm for reflection off the ground and reflection from cloud, based on the tables of calculated 360-nm radiances. For reflection from the ground, the terrain height pressure is used, and the reflectivity is assumed to be 0.08. For cloud radiances, a pressure corresponding to the cloud height from the ISCCP-based climatology is used, and the reflectivity is assumed to be 0.80. The ground and cloud radiances are then compared with the measured radiance. If $I_{ground} \leq I_{measured} \leq I_{cloud}$, and snow/ice is assumed not to be present, an effective cloud fraction f is derived using equation 4:

$$f = \frac{I_{measured} - I_{ground}}{I_{cloud} - I_{ground}} \tag{4}$$

If snow/ice is assumed to be present, then the value of f is divided by 2, based on the assumption that there is a 50-50 chance that the high reflectivity arises from cloud. The decrease in f means that there is a smaller contribution from cloud and a higher contribution from ground with a high reflectivity off snow and ice. Equation 4 is solved for a revised value of I_{ground}, and the ground reflectivity is calculated from equation 3.
The calculated radiances are determined assuming that a fraction f of the reflected radiance comes from clouds with reflectivity 0.80, and a fraction 1-f from the ground, with reflectivity 0.08 when snow/ice is absent and with the recalculated reflectivity when snow/ice is present. An effective Lambertian equivalent reflectivity is derived from the cloud fraction using the following expression:

$$LER = R_g(1-f) + R_c f \tag{5}$$

where R_g is 0.08 when snow/ice cover is assumed to be absent and has the recalculated value when it is assumed present. This reflectivity is not used in the TOMS albedo dataset.
If the measured radiance is less than the ground radiance, then the radiation is considered to be entirely from surface terrain with a reflectivity less than 0.08. The ground reflectivity is then determined by using equation 3. Similarly, if the measured radiance is greater than the cloud radiance, when snow/ice are absent, the reflected radiance is assumed to be entirely

from cloud with reflectivity greater than 0.80, and an R_a derived using the cloud conditions is used in Equation 3 to derive the effective reflectivity. If snow/ice is present, the cloud and ground are assumed to contribute equally to the reflectance at 360 nm. Equation 3 is then used to calculate new values of both ground and cloud reflectivities from these radiances. Radiances at the shorter wavelengths are calculated using these reflectivities and a value of 0.5 for *f*. [4],[7]

6.3 Surface reflectance as measured by MODIS

6.3.1 BRDF model and albedo

The MODIS BRDF/Albedo algorithm consists of two basic steps: atmospheric correction that converts top-of-atmosphere radiance to surface spectral reflectance and bidirectional reflectance distribution function (BRDF) modelling to convert spectral reflectance to spectral albedo.
In order to achieve this, the MODIS BRDF/Albedo product combines registered, multi-date, multi-band, cloud-free, atmospherically corrected surface reflectance data from the MODIS and MISR instruments to a Bidirectional Reflectance Distribution Function in seven spectral bands at a 1 km spatial resolution on a 16-day cycle. From this characterization of the surface anisotropy, the algorithm performs angular integrations to derive intrinsic land surface albedo values for each spectral band and three broad bands covering the solar spectrum.
The albedo values are a directional hemispherical reflectance (black sky albedo) obtained by integrating the BRDF over the exitance hemisphere for a single irradiance direction, and a bihemispherical reflectance (white sky albedo) obtained by integrating the BRDF over all viewing and irradiance directions. Because these albedo values are purely properties of the surface and do not depend on the state of the atmosphere, they can be used with any atmospheric specification to provide true surface albedo as an input to regional and global climate models. [9]

6.3.2 RossThick-LiSparse model

The MODIS BRDF/Albedo algorithm makes use of a linear kernel-based model, the semi-empirical reciprocal RossThick-LiSparse model. Because of the linearity of the model, the grid of model parameters can be averaged to a lower resolution grid, if necessary. Validation of the BRDF model and its performance under conditions of sparse angular sampling and noisy reflectances shows that the retrievals obtained are generally reliable. The solar-zenith angle dependency of albedo may be parameterized by a simple polynomial. The intrinsic land surface albedo values may be used to derive the actual albedo by taking into account the distribution of diffuse skylight.

The BRDF model relies on the weighted sum of an isotropic parameter and two functions (or kernels) of viewing and illumination geometry to determine reflectance *R*:

$$R(\theta,\nu,\phi,\lambda) = f_{iso}(\lambda) + f_{vol}(\lambda)K_{vol}(\theta,\nu,\phi,\lambda) + f_{geo}(\lambda)K_{geo}(\theta,\nu,\phi,\lambda) \qquad (6)$$

where θ, υ and φ are the solar zenith, view zenith and relative azimuth zenith angles; $K_k(\theta, \upsilon,\varphi,\lambda)$ are the model kernels; and $f_k(\lambda)$ are the spectrally dependent BRDF kernel weights or parameters. The kernel weights selected are those that best fit the available observational data. One of these kernels, $K_{vol}(\theta, \upsilon,\varphi,\lambda)$, is derived from volume scattering (as from horizontally homogeneous leaf canopies) radiative transfer models and the other, $K_{geo}(\theta, \upsilon,\varphi,\lambda)$, from

surface scattering and geometric shadow casting theory (as from scenes containing three-dimensional objects that cast shadows and are mutually obscured from view at off-nadir angles). The volume-scattering term expresses effects caused by the small (interleaf) gaps in a canopy whereas the geometric-optical term expresses effects caused by the larger (intercrown) gaps.
Several studies have identified this RossThickLiSparse-Reciprocal kernel combination as the model best suited for the operational MODIS BRDF/Albedo algorithm. From that model the following polynomial has been found to reproduce $\alpha_{bs}(\theta,\lambda)$, the fully modelled black-sky albedo, quite well:

$$\begin{aligned}\alpha_{bs}(\theta,\lambda) = {} & f_{iso}(\lambda)(g_{0iso} + g_{1iso}\theta^2 + g_{2iso}\theta^3) \\ & + f_{vol}(\lambda)(g_{0vol} + g_{1vol}\theta^2 + g_{2vol}\theta^3) \\ & + f_{geo}(\lambda)(g_{0geo} + g_{1geo}\theta^2 + g_{2geo}\theta^3)\end{aligned} \quad (7)$$

Where the g_{jk} coefficients are listed below in table 1, and the $f_k(\lambda)$ are the BRDF model kernel weights or parameters. The integrated coefficients for the white-sky albedo $\alpha_{ws}(\theta,\lambda)$ are also provided.

Term g_{jk} for kernel k	k=Isotropic	k=vol (RossThick)	k=geo (LiSparse-R)
g_{0k}	1.0	-0.007574	-1.284909
g_{1k}	0.0	-0.070987	-0.166314
g_{2k}	0.0	0.307588	0.041840
White-sky	1.0	0.189184	-1.377622

Table 1: Coefficients for the RossThickLiSparse *model shown in equation 7*

Equation 7 works almost perfect for solar zenith angles up to 80 degrees.
The true albedo $\alpha(\theta,\lambda)$, under actual atmospheric conditions can also be modelled quite accurately as an interpolation between the black-sky albedo and white-sky albedo. This is shown in formula 8:

$$\alpha(\theta,\lambda) = \{1 - S(\theta,\tau(\lambda))\}\alpha_{bs}(\theta,\lambda) + S(\theta,\tau(\lambda))\alpha_{ws}(\theta,\lambda) \quad (8)$$

The true albedo is a function of the fraction of diffuse skylight $S(\theta,\tau(\lambda))$, which, in turn, is a function of optical depth τ. [8],[9]

6.3.3 MODIS BRDF/Albedo data product

BRDF parameters are produced via either full or magnitude inversions for every land or coastal area, which is viewed and atmospherically corrected at least once over a 16-day period.
Land areas that remain completely cloud covered over this period are set at fill values. If the majority of days is snow-covered, then the algorithm uses only the snowy pixels to make its retrieval. On the other hand, if only a few days in a period are snow-covered, then they are discarded and a snow-free BRDF retrieval is made.
The quality information associated with the BRDF parameter retrievals reflects the quality of the atmospherically corrected, cloud cleared reflectances used as input, and it reflects the type and stability of the inversion performed. If, because of cloud contamination, there is no clear

MODIS observation acquired during a 16-day period, the corresponding pixel is set to a fill value and is excluded from the computation of the quality factor.
The full inversion does not use a pre-defined BRDF database, but each pixel has a different BRDF shape from the coincident MODIS BRDF/Albedo product.
If insufficient high quality observations are available, due to cloud cover etc., to perform a full inversion, an a priori determination of the shape of the surface BRDF is coupled with the available surface reflectances to derive the surface BRDF and albedo values. This is called magnitude inversion, because it scales the pre-defined BRDF shapes.
The current a-priori MODIS BRDF database was originally derived from the Olsen land cover map and MODIS derived BRDF shapes. The 94 Olsen land cover types have been converted into 24 BRDF appropriate land cover types, from which an example is shown in figure 6.2.
Each BRDF land cover type shares a common BRDF shape that is produced from the MODIS angular observations or ground measurements.
There are 3 layers in the current a-priori MODIS BRDF database. The active season layer represents green vegetation covers. The inactive season layer represents change in vegetation. The snow-covered layer represents the cases covered with snow. [2],[3],[8],[9]

.

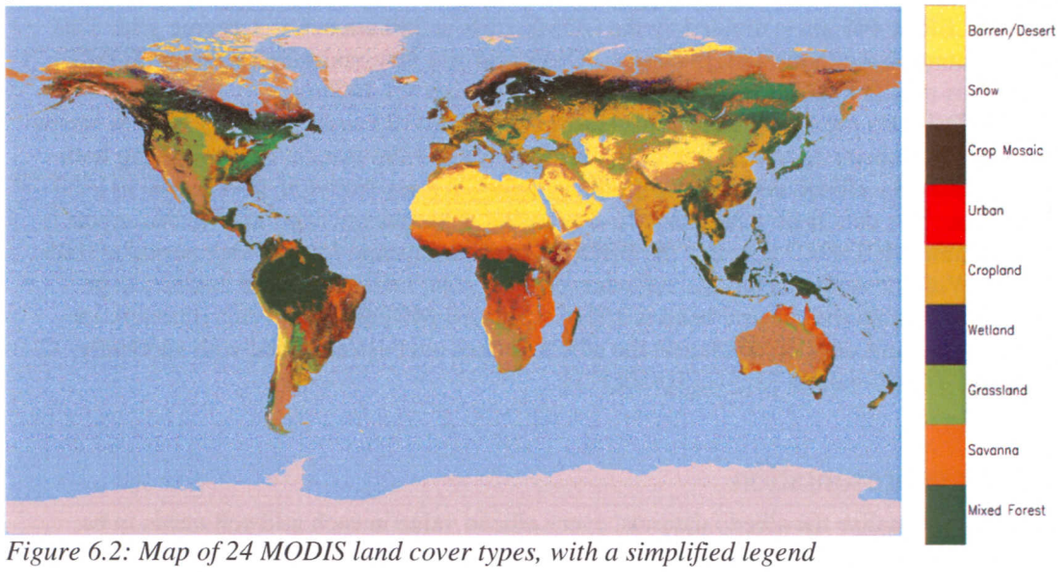

Figure 6.2: Map of 24 MODIS land cover types, with a simplified legend

7 Albedo datasets

7.1 Products

The TOMS dataset is a 1x1.25 degrees gridded Lambertian equivalent reflectivity (LER) map as presented by *Herman and Celarier*. A monthly minimum LER is determined from a 14.5 year's dataset, which covers the period November 1978 – May 1993. The wavelength used in this report is 380 nm. The advantage of the TOMS maps in comparison with the GOME maps is the long measurement series involved and the smaller ground pixel which reduces the problems related to partial cloudiness.
The GOME albedo dataset, used in this report, is a 1x1 degree gridded Lambertian equivalent reflectivity map at wavelength 440 nm as presented by *Koelemeijer et al.*. It covers the period of 27 June 1995 – 31 December 2000. The data is averaged for every month. The advantage of the GOME maps is the very detailed spectral information.
For the NO_2 retrieval, an albedo dataset at 440 nm is needed. The actual albedo dataset for that purpose is based on both TOMS and GOME data. This is done in order to profit from the long dataset from TOMS and the spectral information from GOME. For each month the GOME LER at 440 nm is divided by the GOME LER at 380 nm at a 1x1 degree grid. This ratio is interpolated to the 1x1.25 degree TOMS grid and then multiplied with the TOMS LER. This results in a spectrally corrected TOMS dataset for 440 nm.
The MODIS data products, used in this report, are MOD43B3 and MOD43C2, which can be found at the website of NASA (see [10] and [11]). MOD43B3 is a dataset containing both global black-sky albedo and white-sky albedo values at a resolution of 1/60 degree at local solar noon. The data is obtained for a 16-day period. The spectral band used in this report is 459-479 nm. MOD43C2 contains the BRDF/Albedo parameters for a 16-day period at 0.05 degree. With these parameters the reflectances at all solar and view zenith angles can be determined within the spectral band is 459-479 nm. All MODIS albedo data products are provided for land only. In this report the albedo values over sea are filled with spectrally corrected TOMS values. [3],[4],[5],[10],[11]

7.2 Data presentation

In order to visualise the albedo datasets, every albedo value in each grid cell needs to be coupled with a specific colour. The amount of map colours is set to 256. Albedo values are normalised at 1 and divided into levels. The level width is distributed quadratic, according to $level^2/250^2$. This results in a higher density of levels in the lower range, which is done because albedo values are mostly in the order of 0.03 to 0.2. In this report every albedo value level is mapped at a certain colour, using the following procedure. 250 levels are defined from 0 to 1. In order to get the most contrast where most of the albedo values are situated, a third grade distribution of the colours is chosen empirically. As a criterion is taken that over land, where the most variation in albedo values is, as many as possible albedo values can be distinguished.
It appeared that the colour distribution $\frac{3}{4 \cdot maxcol^2} col^3 - \frac{9}{4 \cdot maxcol} col^2 + \frac{5}{2} col$ gave the most contrast and the largest range of colours over land. *Col* is here the index of the colour, which is a value between 1 and 250. *Maxcol* is the maximum colour index, which is 250 in this case.

7.3 Different resolutions

In order to make the NO_2 retrieval more accurate, an albedo dataset with a higher resolution is desired. Instead of the current 1x1.25 degree albedo dataset, a new dataset should be made at 0.25x0.25 degrees. An even higher resolution would result in a too slow calculation of the NO_2 columns. In order to compare and to combine the different datasets, all datasets are interpolated or averaged at a 0.25x0.25 degree grid. The interpolation is done linear. It results in a smoother image, but the main structures remain the same, as is shown in figure 7.1.

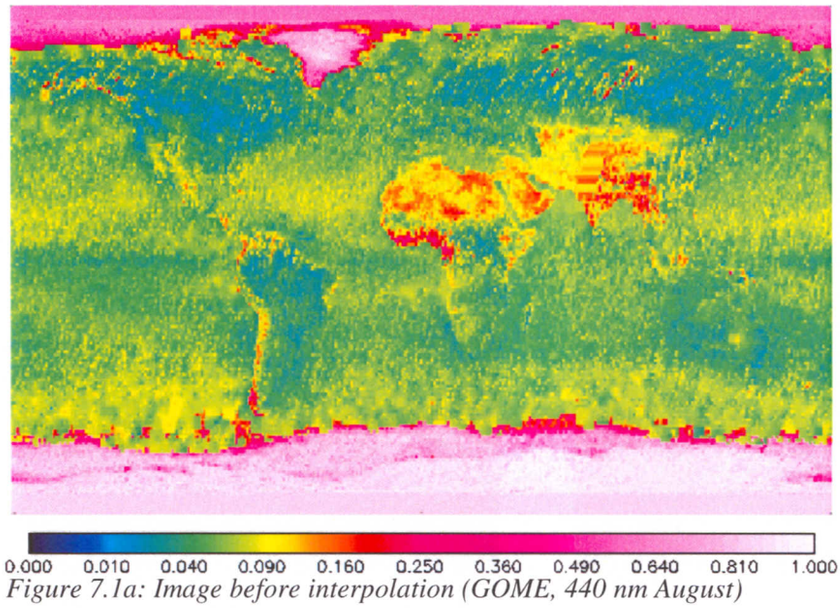

Figure 7.1a: Image before interpolation (GOME, 440 nm August)

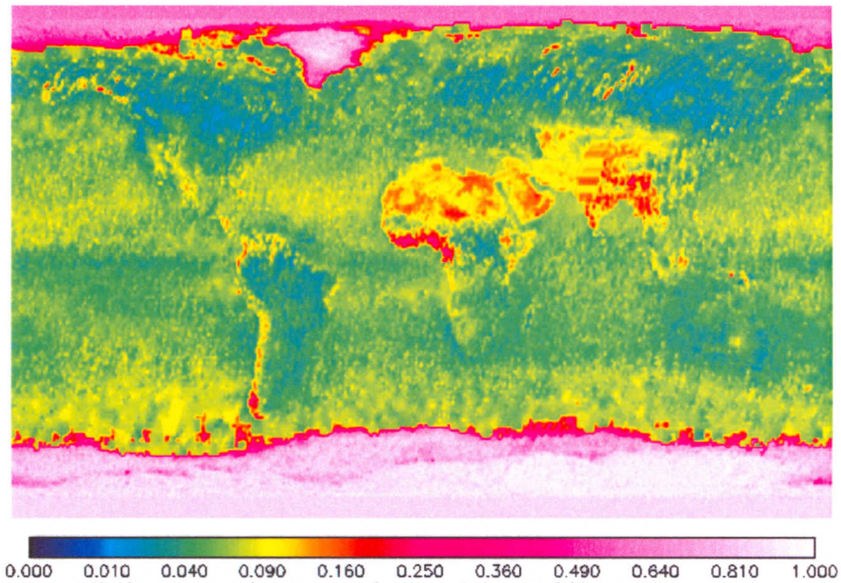

Figure 7.1b: Image after interpolation (GOME, 440 nm August)

The GOME LER data is provided at 1x1 degree grid, while the MODIS black-sky albedo is provided at a 1/60x1/60 degree grid. This 360 times greater amount of pixels results in a large difference in information between both datasets. To illustrate this difference an albedo map for the Benelux is created for both datasets, shown in figure 7.2. Whereas the GOME dataset shows almost no local information, the MODIS dataset shows a lot of detailed structures, for example 'de Veluwe', Westland, the Ardennes, Utrecht, Eindhoven and other cities.

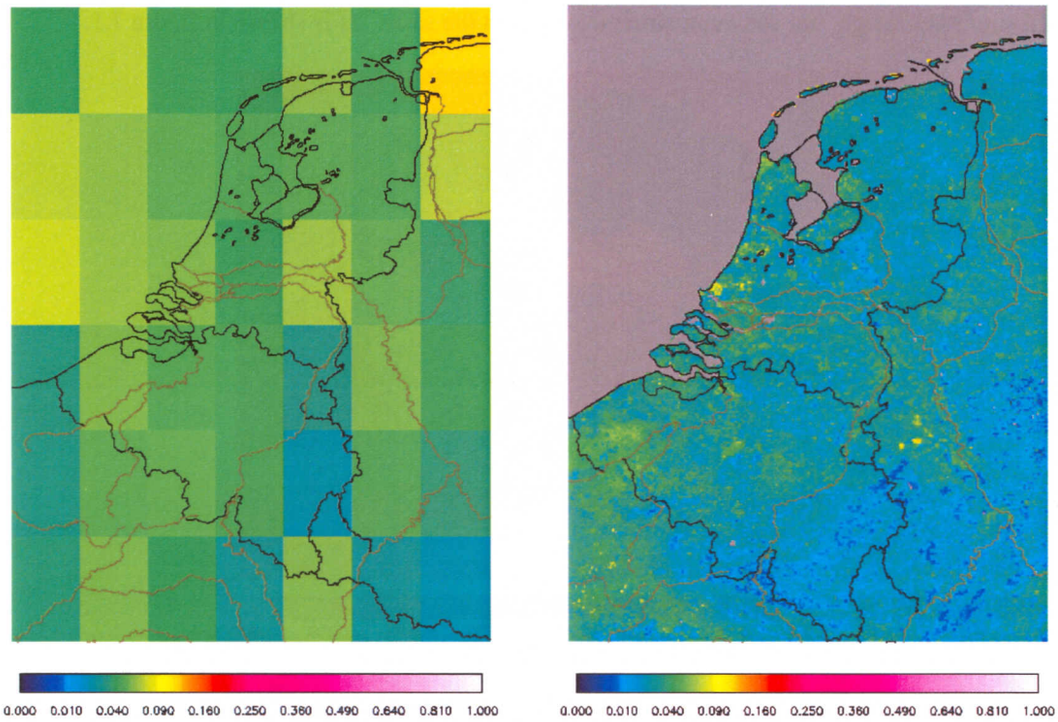

Figure 7.2: Resolution difference between GOME (left) and MODIS (right)

8 Albedo datasets comparison

8.1 Comparison MODIS white-sky and black-sky albedo

The true albedo can be expressed as a linear combination of the black-sky albedo and the white-sky albedo. If there would be none or very little difference between both datasets, it is not necessary to take a linear combination. In that case the true albedo can be approximated by the black-sky albedo, because in the case of 440 nm about 80% of the illumination is direct. That is why is investigated whether there are differences between the MODIS black-sky and the MODIS white-sky albedo values at the wavelength of 460 nm. For the month of August the black-sky albedo and the white-sky albedo are imaged in figure 8.1.

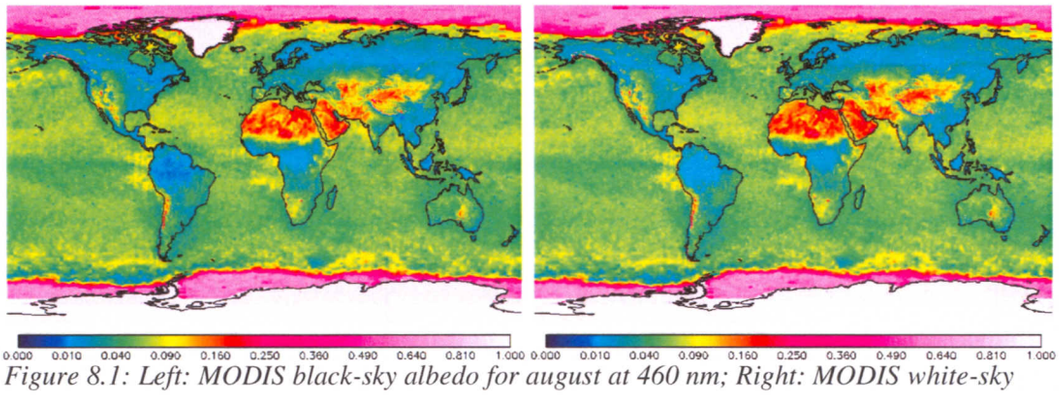

Figure 8.1: Left: MODIS black-sky albedo for august at 460 nm; Right: MODIS white-sky albedo for august at 460 nm

From figure 8.1 it appears that there is little difference between both datasets. In order to quantify this, a ratio of the white-sky albedo divided by the black-sky albedo is determined. This is done for the month of August for every pixel at a 0.25x0.25 degree grid. The result is imaged in figure 8.2a. The scale of the ratio images in this report is the same for all comparisons.

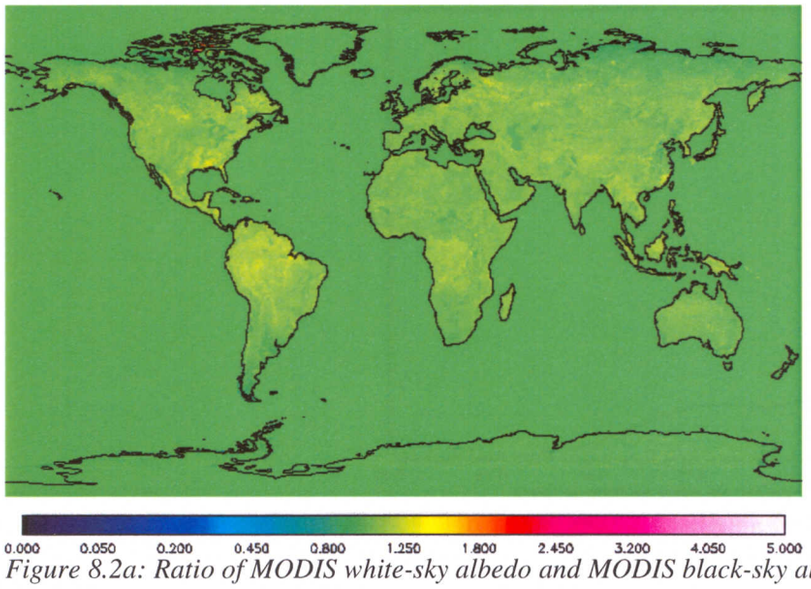

Figure 8.2a: Ratio of MODIS white-sky albedo and MODIS black-sky albedo at 460 nm

Over sea the ratio is 1, because it is filled with spectrally corrected TOMS values in both cases. Over land the ratio varies between 1.0 and 1.2, where the 1.2 values are mainly found over the rainforests. The mean value over land is 1.07±0.06. So the white-sky albedo values are on average 7% percent higher than the black-sky albedo values.

In order to investigate for which albedo values the difference is largest, the mean difference per albedo value is plotted in figure 8.2b. In figure 8.2c the albedo distribution is plotted. It appears that the larger the albedo values, the larger the differences. From figure 8.2c is inferred that most albedo values are situated between 0.01 and 0.09. In this range the albedo values differ less than 0.007. A smaller, but still a significant, part of the albedo values is situated in the range from 0.09 to 0.18. There the differences vary between 0.007 and 0.012. It is concluded that the true albedo can be approximated by the black-sky albedo, because of the small differences for most albedo values and because about 80% percent of the illumination is direct. [10]

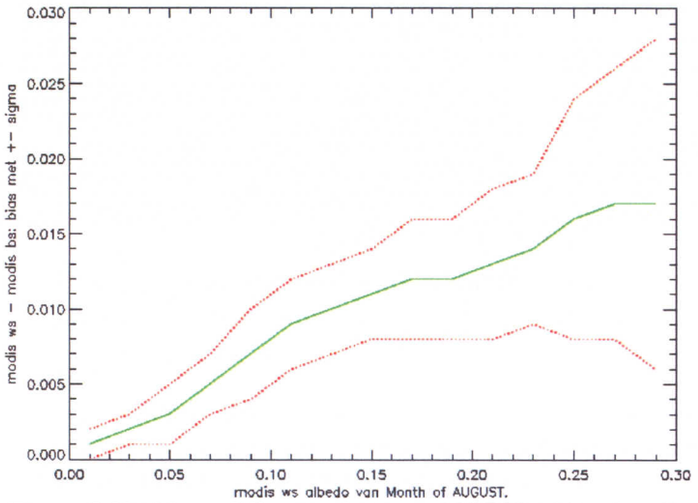

Figure 8.2b: Mean difference between MODIS white-sky albedo and MODIS black-sky albedo at 460 nm (green) and its sigma (red) as a function of albedo

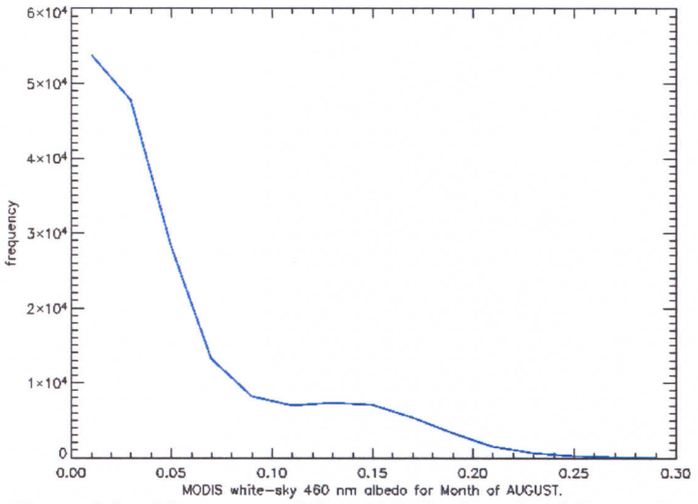

Figure 8.2c: Histogram of the MODIS white-sky 460 nm albedo distribution

8.2 Comparison GOME 440 nm and 380 nm

It is important to have knowledge about the difference between the GOME LER at 440 nm and at 380 nm, because the ratio of them is used in the current albedo dataset as a wavelength correction. In order to investigate whether this ratio is a significant factor and to what extent the albedo is wavelength dependent, the ratio of the GOME LER at 440 nm divided by the GOME LER at 380 nm is calculated. This is performed for the month of August for every pixel at a 0.25x0.25 degree grid. The result is imaged in figure 8.3a.
It appears that over sea there is little difference between both datasets. The ratio varies mainly between 0.8 and 1.2, while most values are very close to 1. The overall mean ratio is 1.1 with a sigma of 0.3. Over land the mean ratio is 1.6 with a sigma of 0.3, which shows that there is a significant difference between the datasets. The lowest ratios are primarily found over terrains with relative low land albedo, like rainforests in South America, Central Africa and Southeast Asia.

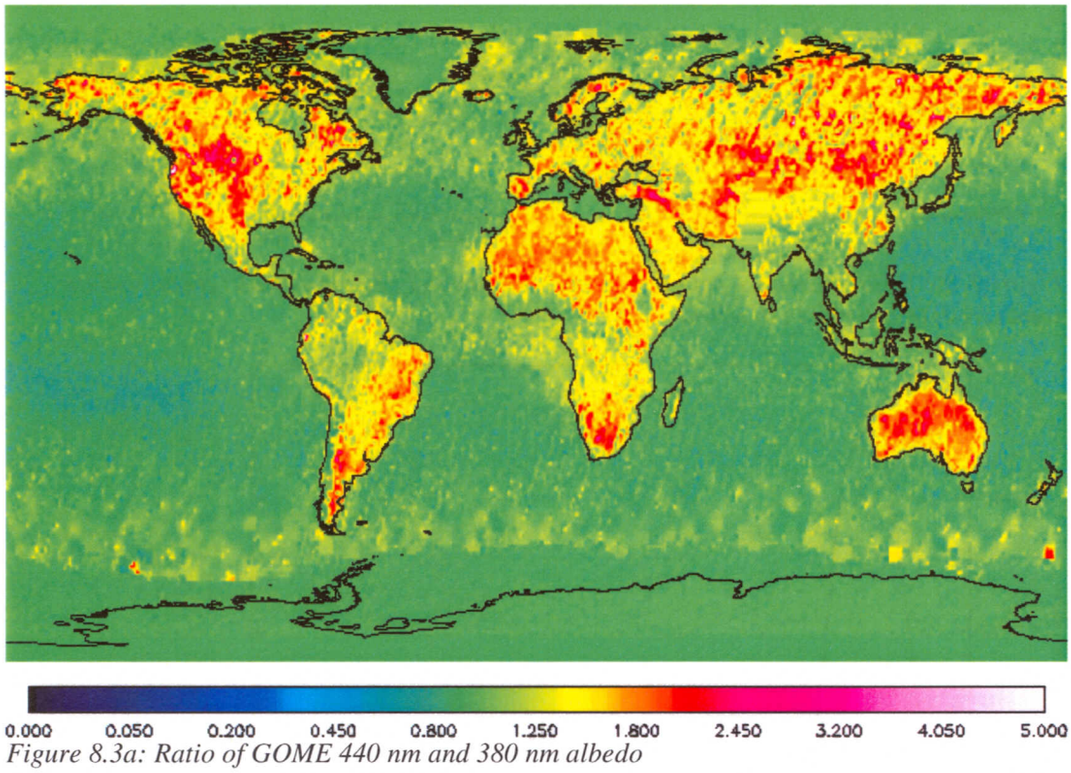

Figure 8.3a: Ratio of GOME 440 nm and 380 nm albedo

In order to investigate for which albedo values the largest differences exist, the mean difference per albedo value is plotted in figure 8.3b. In figure 8.3c the albedo distribution is plotted. Maximum frequencies are about 19000. Therefore, albedo values with a frequency less than 50 are omitted. The South Pole is omitted as well. Due to the snow and ice contamination, it will not contribute to significant differences.

It appears that the largest differences occur for albedo values between 0.1 and 0.2. However, from figure 8.3c is inferred that most albedo values are situated between 0.03 and 0.08. In that range however, the difference is smallest. There the albedo values differ less than 0.005.
It is concluded that the ratio used in the current dataset is a significant factor, especially for land albedo values between 0.1 and 0.2, and thus can not be ignored.

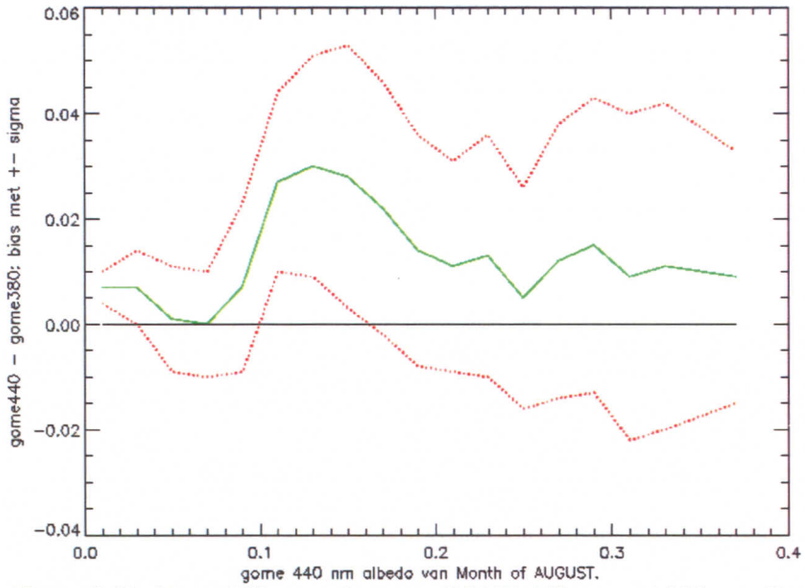

Figure 8.3b: Mean difference between GOME 440 nm and 380 nm albedo (green) and its sigma (red) as a function of albedo

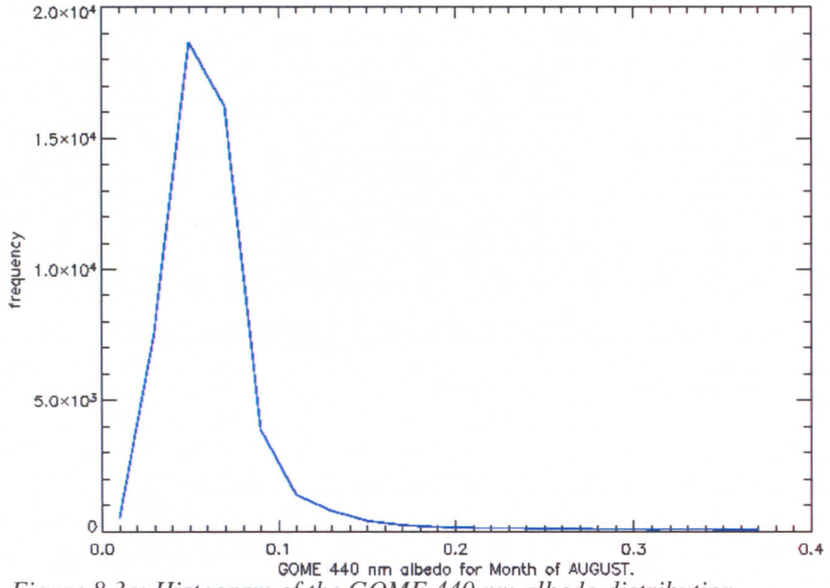

Figure 8.3c: Histogram of the GOME 440 nm albedo distribution

8.3 Comparison GOME 440 nm and 463 nm

All MODIS albedo data products are provided at wavelengths larger than 440 nm. The spectral band with the smallest wavelengths is centred at 469 nm. From chapter 8.2 it appeared that the wavelength difference between 440 nm and 380 nm had significant influence on the albedo. Therefore is investigated whether the smaller difference in wavelength between 440 nm and 469 nm is significant as well for the albedo.
In order to do this, a ratio is determined of the GOME LER at 440 nm divided by the GOME LER at 463 nm. This is done for the month of August for every pixel at a 0.25x0.25 degree grid. The result is imaged in figure 8.4a.
Over sea the ratio shows that there is a small difference between the datasets. The ratio there appears to be between 1.2 and 1.3. The overall mean ratio is 1.06 with a sigma of 0.08. Over land the mean ratio is 0.97 with a sigma of 0.05. The rainforests in South America, Africa and Indonesia have a little higher ratio of about 1.1. So there is mainly no difference between the albedo over land at 440 nm and at 463 nm. The small difference over sea has no influence, because there is no MODIS albedo data over sea. The MODIS albedo of the rainforests might be until 10% higher at 440 nm than the value determined at 469 nm.

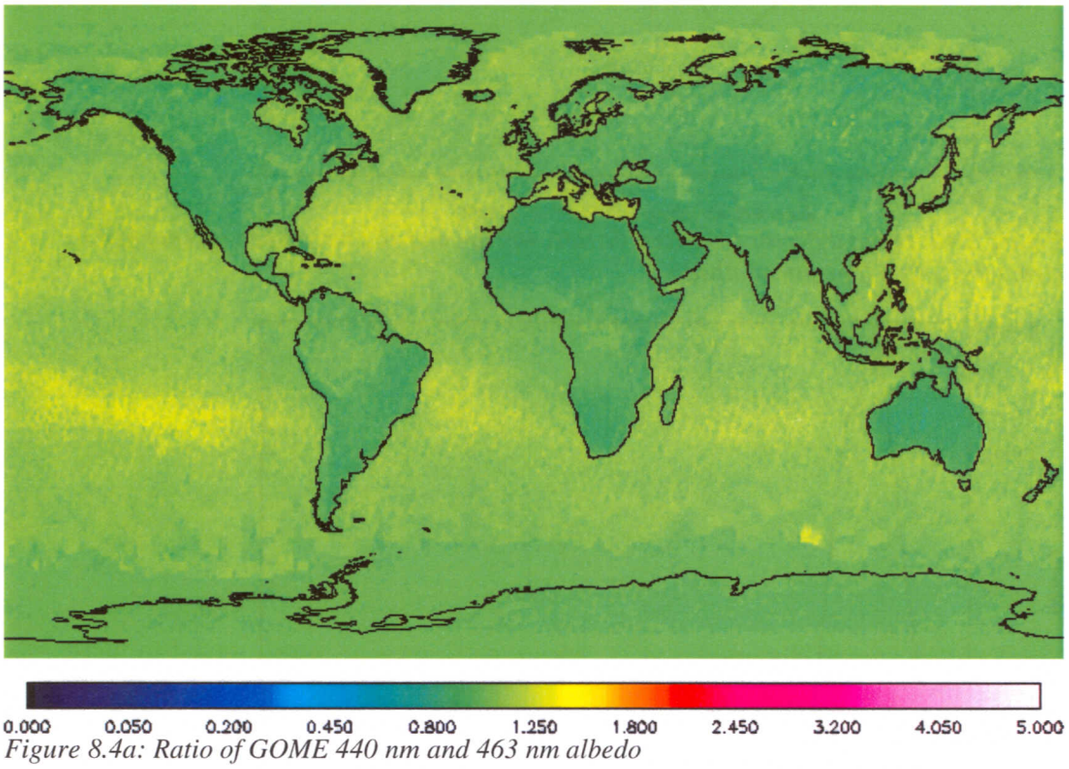

Figure 8.4a: Ratio of GOME 440 nm and 463 nm albedo

In order to investigate for which albedo values the difference is largest, the mean difference per albedo value is plotted in figure 8.4b. In figure 8.4c the albedo distribution is plotted for the GOME 440 nm dataset. Maximum frequencies are about 19000. Therefore albedo values with a frequency less than 50 are omitted. The South Pole is omitted as well. Due to the snow and ice contamination, it will not contribute to significant differences.

It appears that the largest differences occur for albedo values between 0.05 and 0.16, as well positive as negative. From figure 8.4c is inferred that most albedo values are situated between 0.03 and 0.08. In this range the albedo values differ less than 0.005.
It is concluded that most differences are less than 0.005, so the 469 nm albedo MODIS dataset can be used for comparisons with other datasets at 440 nm. However, a wavelength correction would locally give slightly more accurate values.

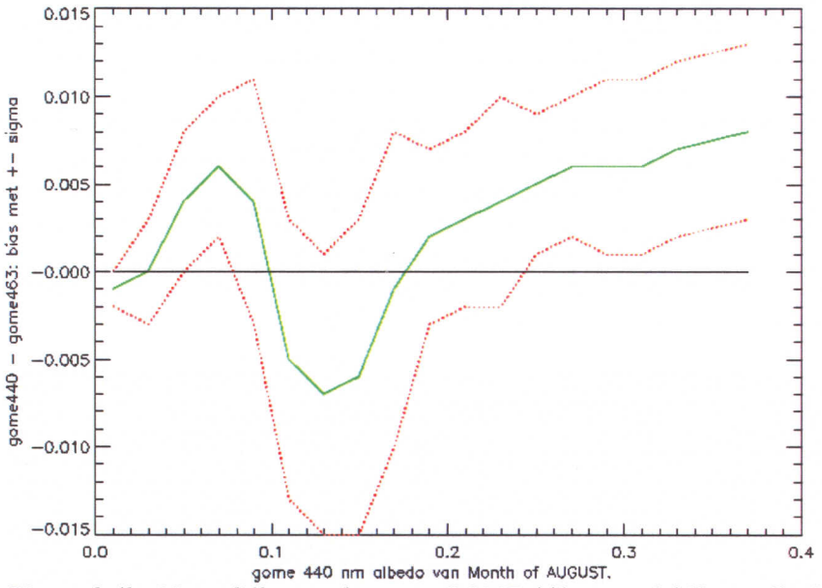

Figure 8.4b: Mean difference between GOME 440 nm and 463 nm albedo (green) and its sigma (red) as a function of albedo

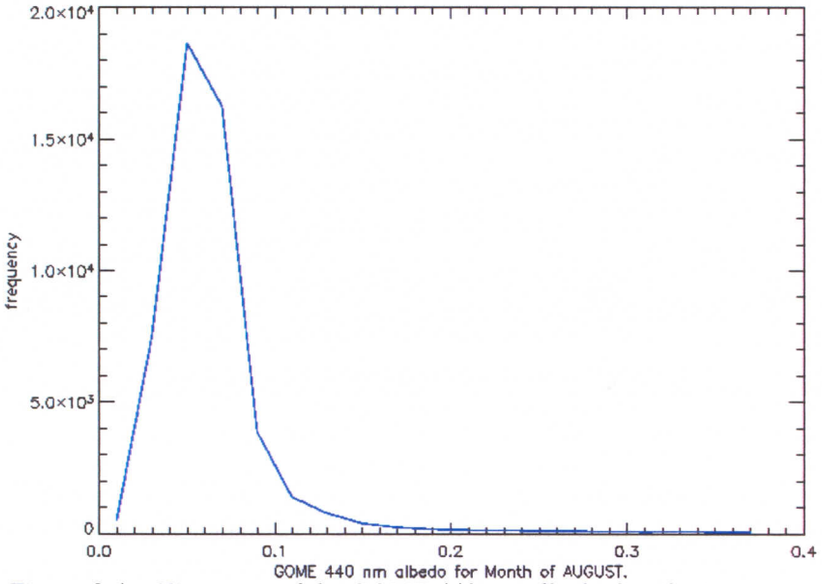

Figure 8.4c: Histogram of the GOME 440 nm albedo distribution

8.4 Comparison TOMS and GOME

The GOME dataset is used for a spectral correction on the TOMS dataset. In order to compare the spectrally corrected TOMS dataset with the GOME dataset, the ratio is determined of the TOMS LER at 440 nm divided by the GOME LER at 440 nm. This is done for the month of August for every pixel at a 1x1.25 degree grid. The result is imaged in figure 8.5a.
Over sea there are small differences. The ratio varies between 0.6 and 1.5, but averages at 1. The overall mean ratio is 1.2 with a sigma of 0.9. Over land there are quite large differences between both datasets. The mean ratio over land is 1.0 with a sigma of 0.4. Over Europe, Asia and North America the ratio varies mainly between 1.0 and 2.5, while most ratio values are about 1.5. However, over the west coast of Africa and over India the ratio varies between 0.1 and 0.6.

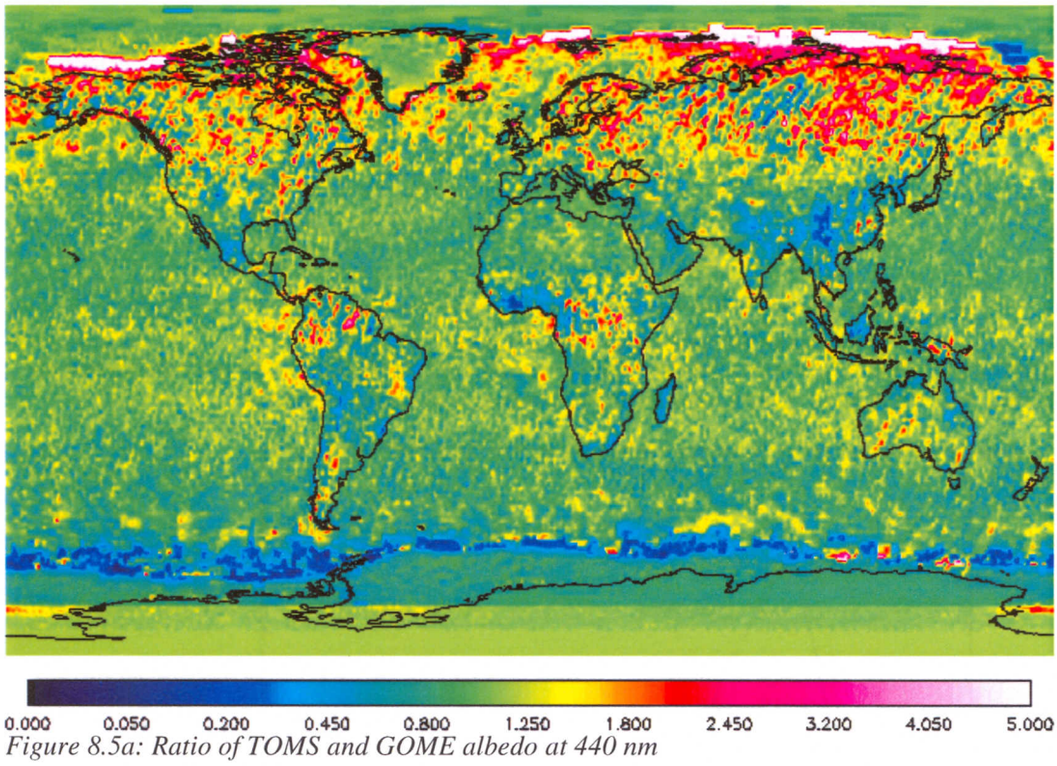

Figure 8.5a: Ratio of TOMS and GOME albedo at 440 nm

In order to investigate for which albedo values the difference is largest, the mean difference per albedo value is plotted in figure 8.5b. In figure 8.5c the albedo distribution is plotted. Maximum frequencies are about 16000. Therefore albedo values with a frequency less than 50 are omitted. The South Pole is omitted as well. Due to the snow and ice contamination, it will not contribute to significant differences.

It appears that the largest significant differences occur for albedo values between 0.01 and 0.03. From figure 8.5c is inferred that most albedo values are between 0.03 and 0.09. In this range the albedo values differ less than 0.01
Concluded is that GOME albedo values are on average quite similar to spectrally corrected TOMS albedo values. For low albedo values, like over India and the west coast of Africa, GOME gives slightly higher albedo values.

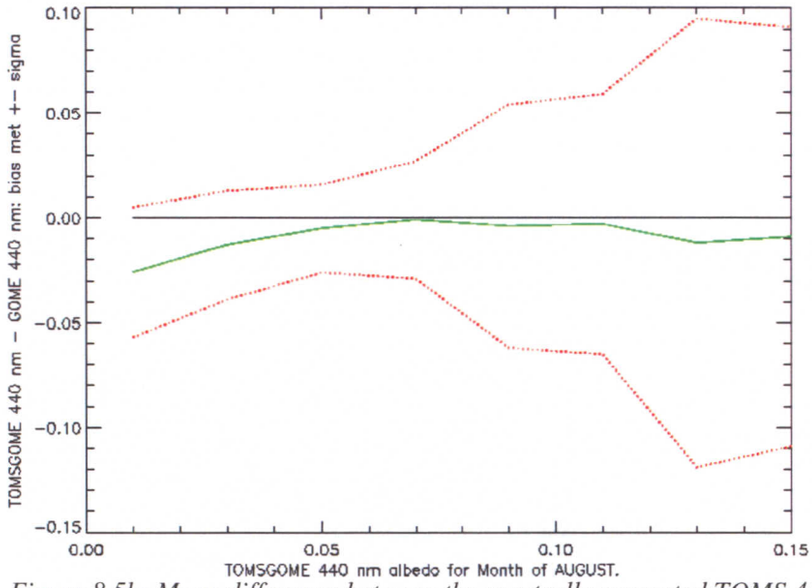

Figure 8.5b: Mean difference between the spectrally corrected TOMS 440 nm albedo and the GOME 440 nm albedo (green) and its sigma (red) as a function of albedo

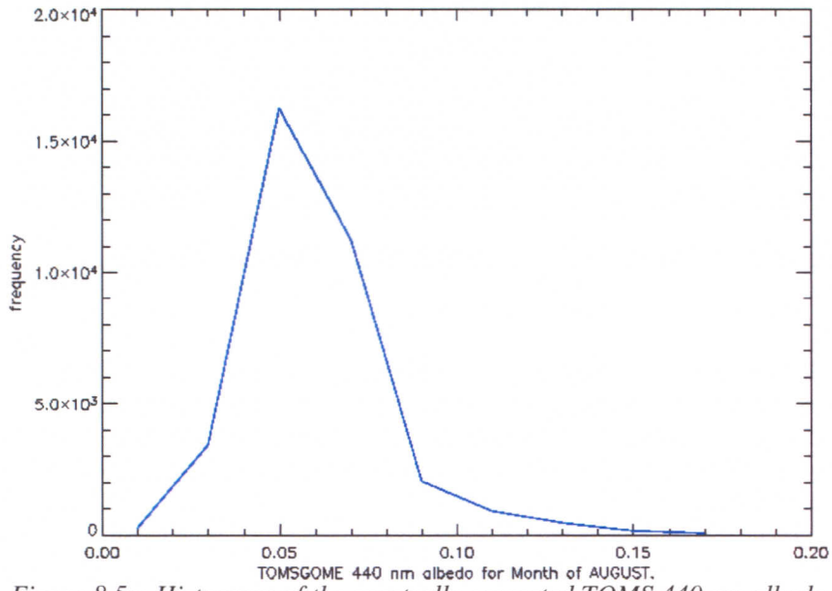

Figure 8.5c: Histogram of the spectrally corrected TOMS 440 nm albedo distribution

8.5 Comparison TOMS and MODIS

Differences between the current TOMS albedo dataset and the MODIS albedo dataset would have direct effect on the determined NO_2 concentrations. In order to investigate the difference between these datasets, the ratio of TOMS at 440 nm and MODIS black-sky is determined. This is done for the month of August for every pixel at a 0.25x0.25 degree grid. The result is imaged in figure 8.6a.
The mean ratio over land appears to be 1.9 with a sigma of 1.5. The sea values in the MODIS map are filled with values from the current albedo dataset, therefore the ratio over sea is 1. Over land there are large differences between both datasets. Over dry areas and deserts the ratio varies between 0.4 and 1.0, while most values are about 0.5. So in those areas the MODIS albedo is about 2 times higher. Over Asia, Europe and North America the MODIS albedo values are persistently about 3 times lower. Over the rainforests in South America, Central Africa, Indonesia and Southeast Asia the ratio varies mainly between 3 and 5, where all ratio values higher than 5 are truncated at 5, but most values in those areas are not much higher than 5.

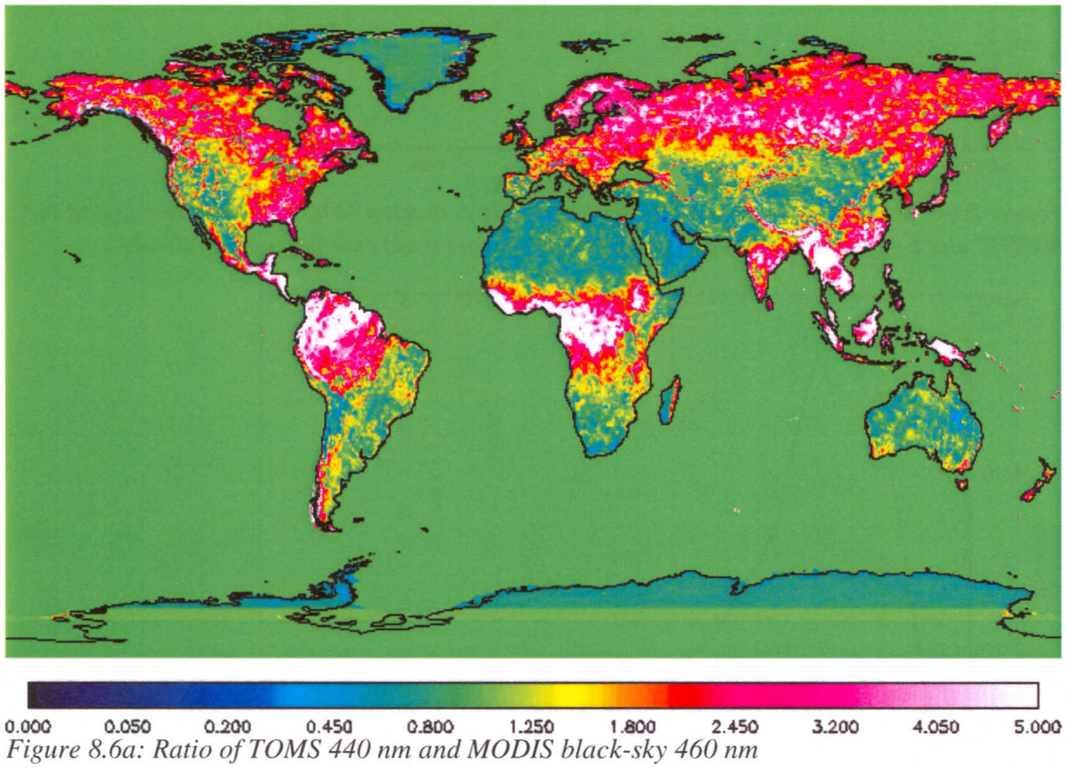

Figure 8.6a: Ratio of TOMS 440 nm and MODIS black-sky 460 nm

In order to investigate for which albedo values the difference is largest, the mean difference per albedo value is plotted in figure 8.6b. In figure 8.6c the albedo distribution is plotted. Maximum frequencies are about 60000. Therefore albedo values with a frequency less than 50 are omitted. The South Pole is omitted as well. Due to the snow and ice contamination, it will not contribute to significant differences.

It appears that the largest significant differences occur for albedo values between 0.03 and 0.08. From figure 8.6c is inferred that most albedo values are between 0.02 and 0.10. In this range the differences are largest, until 0.02 on average, which is relatively large with respect to the low albedo values. Concluded is that TOMS and MODIS have large differences, especially for low albedo values. [10]

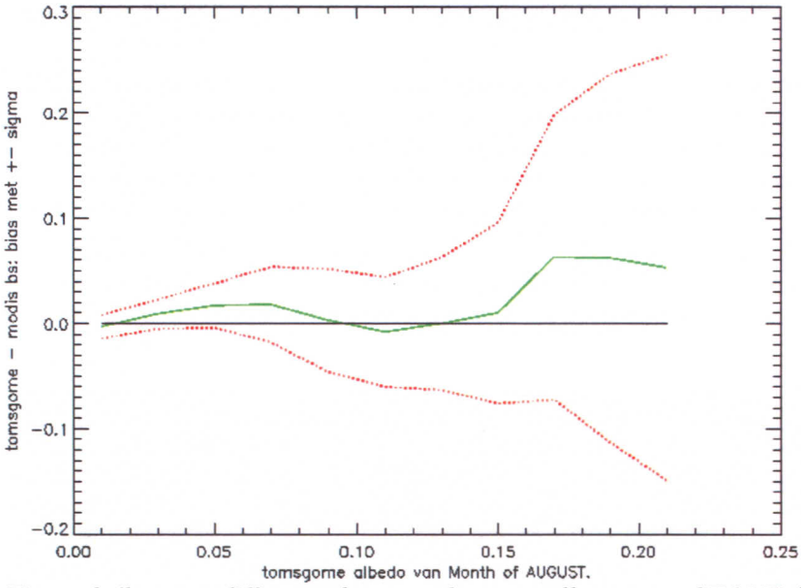

Figure 8.6b: mean difference between the spectrally corrected TOMS 440 nm albedo and the MODIS black-sky 460 nm albedo (green) and its sigma (red) as a function of albedo

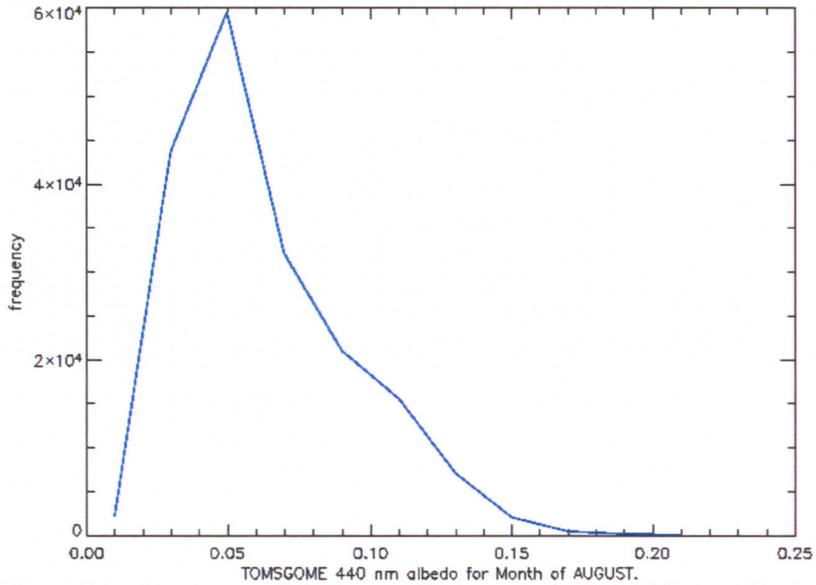

Figure 8.6c: histogram of the spectrally corrected TOMS 440 nm albedo distribution

8.6 Comparison MODIS black-sky albedo and custom geometry reflectance

The NO_2 retrieval does not require a surface albedo map, but a surface reflectance map. The MODIS BRDF parameters can be used to model the surface reflectance at a custom geometry. In order to perform this, a user tool is made available on the website of Boston University. This tool is rewritten to a FORTRAN function. Using this function, a dataset with local solar angles for SCIAMACHY and a dataset with the MODIS BRDF parameters, a global reflectance map is created for a viewing direction in nadir for the SCIAMACHY geometry. This is performed for 2 16-day periods, starting at day number 65 and at day number 161. The results are compared with the corresponding black-sky albedo maps.
In figure 8.7a the MODIS black-sky albedo is imaged for the 16-day period starting at day 65 averaged for 2000-2004. Figure 8.7b shows the reflectance map for the 16-day period starting at day 65 in 2000 for the SCIAMACHY geometry. Figure 8.8a and 8.8b show the same scenes for the 16-day period starting at day 161. For reference the spectrally corrected TOMS albedo dataset at 440 nm for June is imaged in figure 8.8c.

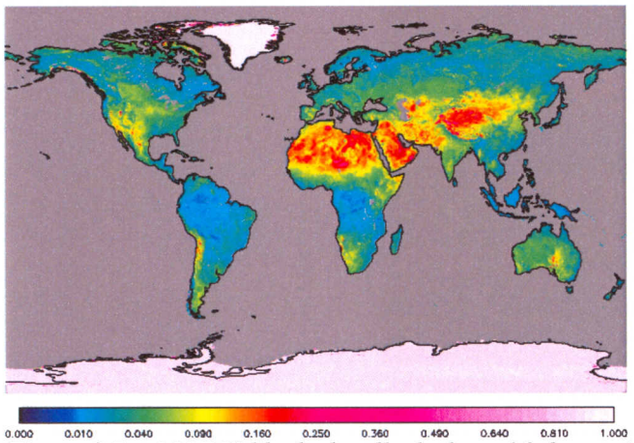

Figure 8.7a: MODIS black-sky albedo for a 16-day period starting at day 65 averaged for 2000-2004

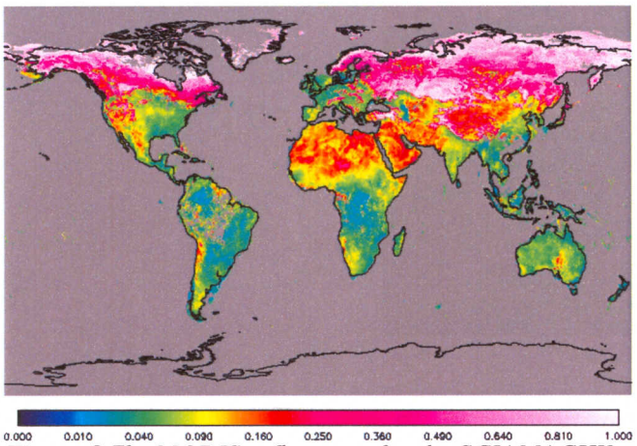

Figure 8.7b: MODIS reflectance for the SCIAMACHY geometry for a 16-day period starting at day 65 for nadir viewing angle

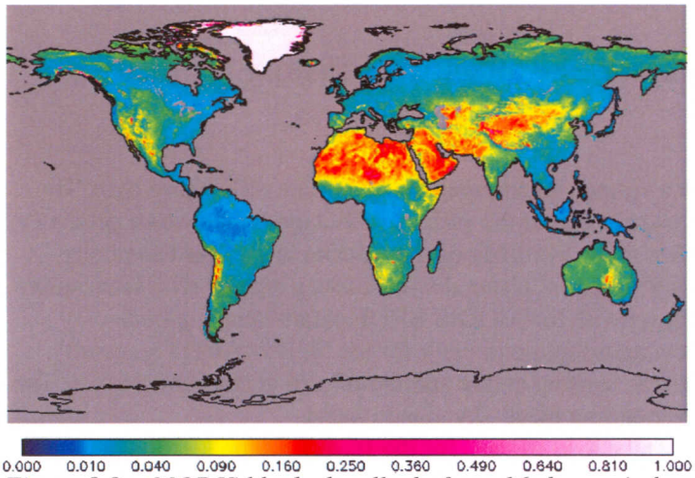

Figure 8.8a: MODIS black-sky albedo for a 16-day period starting at day 161 averaged for 2000-2004

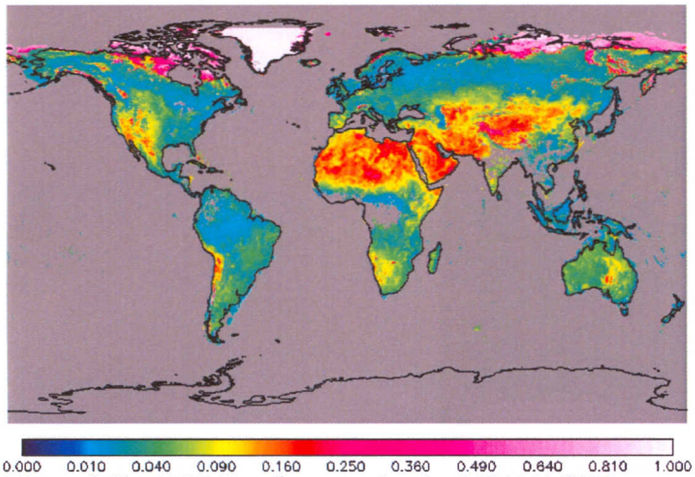

Figure 8.8b: MODIS reflectance for the SCIAMACHY geometry for a 16-day period starting at day 161 for nadir viewing angle

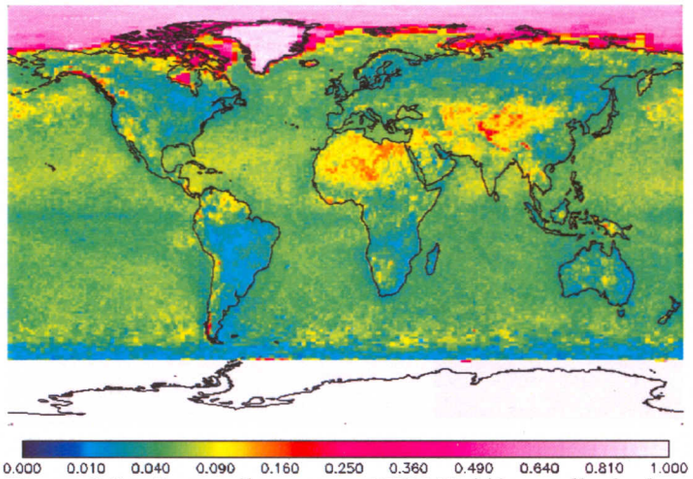

Figure 8.8c: Spectrally corrected TOMS 440 nm albedo dataset for the month of June

From both periods the same characteristics become visible. In comparison with the MODIS black-sky albedo maps, the custom reflectance maps show a lot of snow and cloud contamination. The custom reflectance maps also have until 0.01 higher values, but show mainly similar characteristics.

In order to quantify the differences between the reflectance for the SCIAMACHY geometry and the MODIS black-sky albedo, the ratio of them is determined. This is performed for a 16-day period starting at day 65 (figure 8.9a) and a 16-day period starting at day 161 (figure 8.9b) for every pixel at a 0.25x0.25 degree grid.

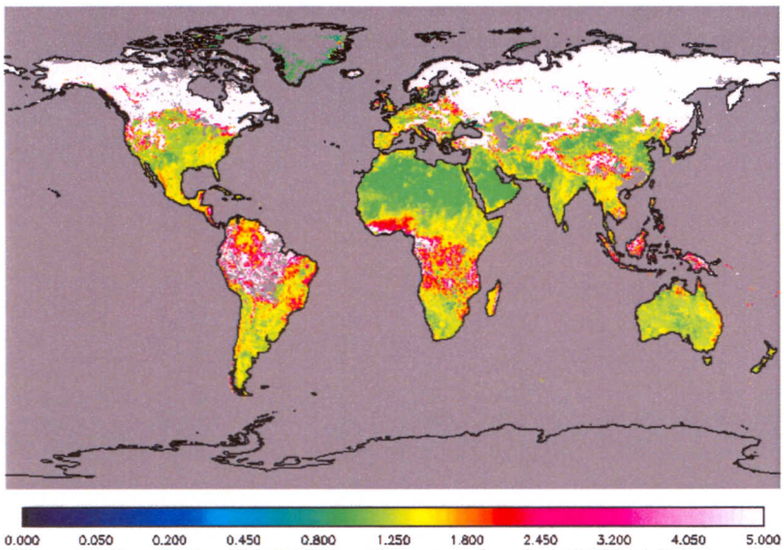

Figure 8.9a: Ratio of MODIS reflectance for the SCIAMACHY geometry for nadir viewing direction and MODIS black-sky albedo averaged for 2000-2004 for a 16-day period starting at day 65

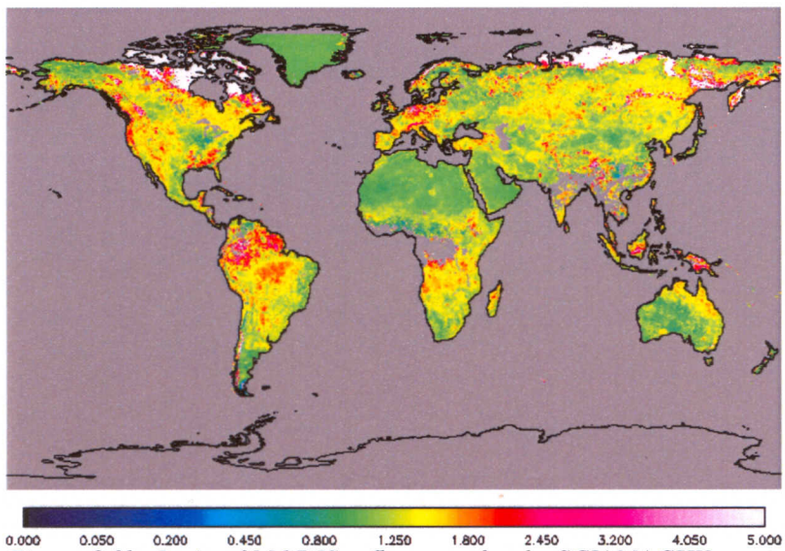

Figure 8.9b: Ratio of MODIS reflectance for the SCIAMACHY geometry for nadir viewing direction and MODIS black-sky albedo averaged for 2000-2004 for a 16-day period starting at day 161

Due to the large cloud and snow contamination, only part of the maps is useful for comparison. The ratio is globally situated between 1.0 and 1.5, where the lowest ratios are situated over areas with relatively high albedo values. The mean ratio is determined only for areas without snow or cloud contamination. For both periods the mean ratio appeared to be 1.27 with a sigma of 0.24.
The reflectance values are on average 27% larger than the black-sky albedo values. So it is concluded that the MODIS black-sky albedo is an overestimation of the reflectance for SCIAMACHY geometry. However for the NO_2 retrieval, it is a good approximation of the MODIS reflectance map, because the differences are small in comparison with the large differences with the current albedo dataset. The differences are explained by the fact that the albedo can be considered as an averaged reflectance over all view angles. Therefore the albedo is a good approximation of the reflectance, but in a lot of cases they are different. [10],[11]

9 Application in NO_2 retrieval

NO_2 columns are retrieved with a precision of 35-60% over heavy polluted regions, like large parts of Europe, USA and China. This uncertainty largely proceeds from the uncertainty in the air mass factor. The surface albedo is responsible for an uncertainty in the air mass factor of 15%. Therefore a change in albedo would also give a significant change in the air mass factor and therefore in the NO_2 column. [1]

9.1 NO_2 columns change estimation

The dependency of the tropospheric air mass factor on the surface albedo is imaged in figure 9.1.

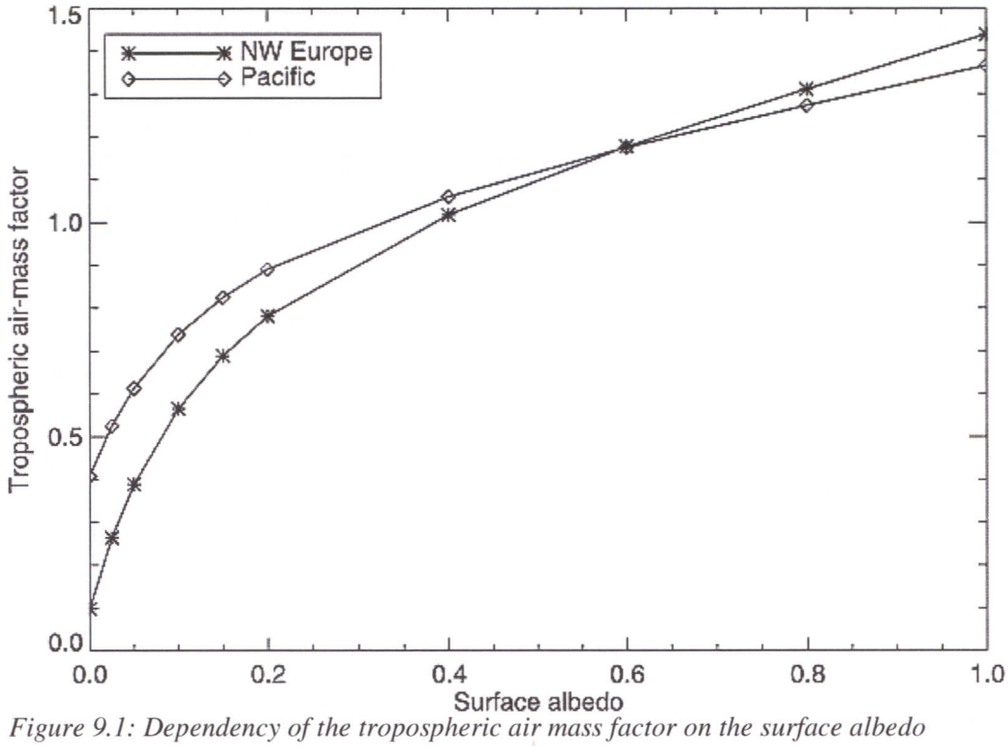

Figure 9.1: Dependency of the tropospheric air mass factor on the surface albedo

It results from figure 9.1 that a change in albedo affects the tropospheric air mass factor at most for small albedo values.

The dependency of air mass factor M on surface albedo a_{sf}, $\frac{\partial M}{\partial a_{sf}}$, is about 3.5 for polluted areas and about 2.5 for clean areas, for albedo values less than 0.2, as appears from figure 9.1. Over Northwest Europe the TOMS LER is on average about 0.05. For MODIS black-sky albedo this is about 0.03. Therefore, if the MODIS black-sky albedo is used instead of the TOMS LER, the albedo will be 0.03 instead of 0.05. From figure 9.1 it is determined that this will lead to a decrease in the tropospheric air mass factor from 0.37 to 0.3. This decrease will cause the NO_2 column value to increase with a factor 1.23. [1]

9.2 NO_2 columns compared

The effect of using the MODIS black-sky albedo dataset for the NO_2 retrieval instead of the current TOMS LER dataset is investigated. For this purpose, a NO_2 retrieval is performed for both datasets in order to obtain the total and the tropospheric columns for July 1998. The tropospheric columns are determined by using model NO_2 values for the stratosphere, which are subtracted from the total column values.

9.2.1 Total NO_2 columns

The result for the total column values is imaged in figure 9.2. The left image shows the determined total NO_2 column values for the case that the spectrally corrected TOMS LER dataset is used and the right image shows the case that the MODIS dataset is used.

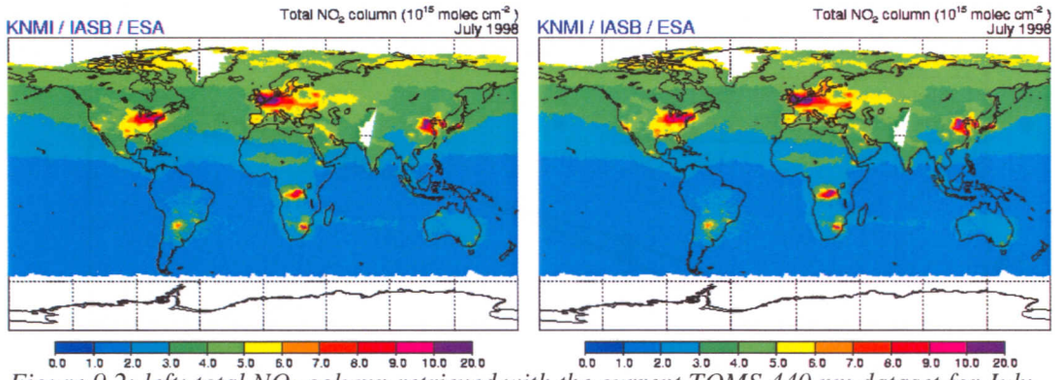

Figure 9.2: left: total NO_2 column retrieved with the current TOMS 440 nm dataset for July 1998; right: total NO_2 column retrieved with the MODIS black-sky 460 nm dataset for July 1998

From figure 9.2 no clear differences between both cases are visible. In order to quantify the differences, a ratio of the images is calculated. This is performed by dividing the total column values for MODIS by the total column values for TOMS. The result is shown in figure 9.3.

It appears that almost every value is situated between 0.95 and 1.05, except in Central Africa. There the ratio varies between 1.08 and 1.25. Over Saudi Arabia, South Africa and the northern of Australia the ratio is about 0.95. Over the eastern of the USA and over Northwest Europe the ratio varies mainly between 1.01 and 1.05. Over sea the ratio is largely 1. Concluded is that the total column values are affected by using the MODIS albedo dataset with about 5%, as well positive as negative.

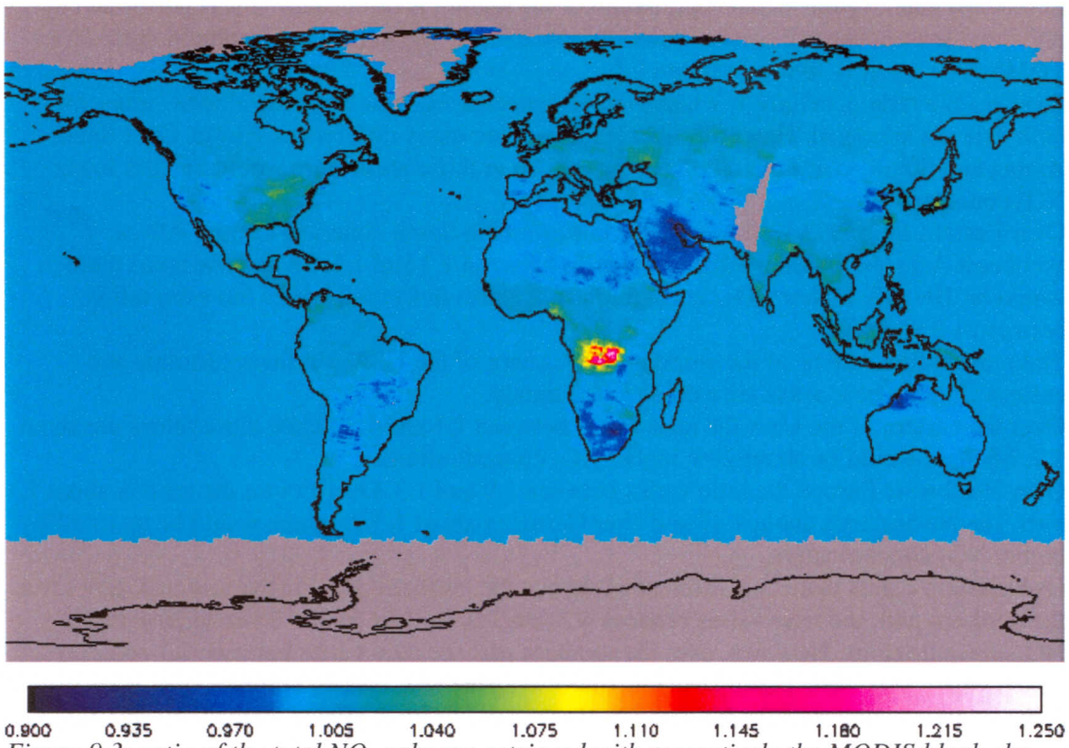

Figure 9.3: ratio of the total NO_2 columns retrieved with respectively the MODIS black-sky 460 nm albedo and the current TOMS 440 nm dataset for July 1998

9.2.2 Tropospheric NO_2 columns

The result for the tropospheric column values is imaged in figure 9.4. The left image shows the determined tropospheric NO_2 column values for the case that the TOMS dataset is used and right image for the case that the MODIS dataset is used. In these images more empty pixels are visible due to cloud contamination. For the total column value map, these pixels are filled with model values.

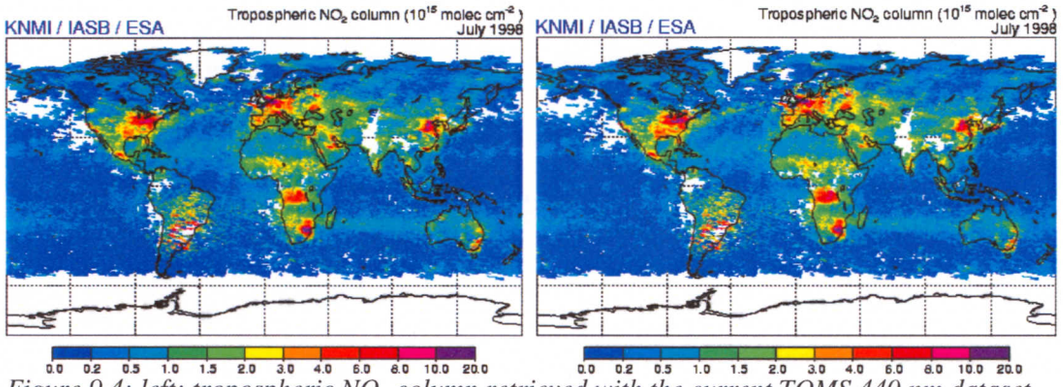

Figure 9.4: left: tropospheric NO_2 column retrieved with the current TOMS 440 nm dataset for July 1998; right: tropospheric NO_2 column retrieved with the MODIS black-sky 460 nm dataset for July 1998

In order to quantify the differences, a ratio of the images is calculated. This is performed by dividing the tropospheric column values for MODIS by the tropospheric column values for TOMS. The result is shown in figure 9.5.
Over sea the ratio is mainly 1, which is to be expected, because there the albedo values for both datasets are equal. However, over land there are many differences visible. Over Saudi Arabia and South Africa the ratio is about 0.8. So in those areas there would be 20% lower NO_2 concentrations.
Over Eastern Europe as well as over the rainforests in South America, Central Africa, Southeast Asia and Indonesia the ratio varies between 1.1 and 1.3. So in those areas there would be 10–30% higher NO_2 concentrations. An area in Central Africa has even ratios between 1.3 and 1.5.
The most polluted areas of the world are the eastern of the USA, Northwest Europe and eastern China. These areas are examined separately.
Over the eastern of the USA the ratio varies between 1.1 and 1.3, while most values are about 1.2. So there would be about 20% higher NO_2 concentrations.
Over Northwest Europe the ratio varies between 1.0 and 1.3. Over France the ratio is about 1, over The Netherlands about 1.15 and over Germany about 1.3. So there would be up to 30% higher NO_2 concentrations.
Over eastern China there is a difference between the northern part and the southern part. Over the northern part, the ratio varies between 0.8 and 1.0, so there would be up to 20% lower NO_2 concentrations. However, over the southern part the ratio varies between 1.1 and 1.3, which means that there would be about 10-30% higher NO_2 concentrations.
It is concluded that using the MODIS albedo dataset has large effects on the tropospheric NO_2 column values. The mostly polluted areas of the world appear to be even more polluted.

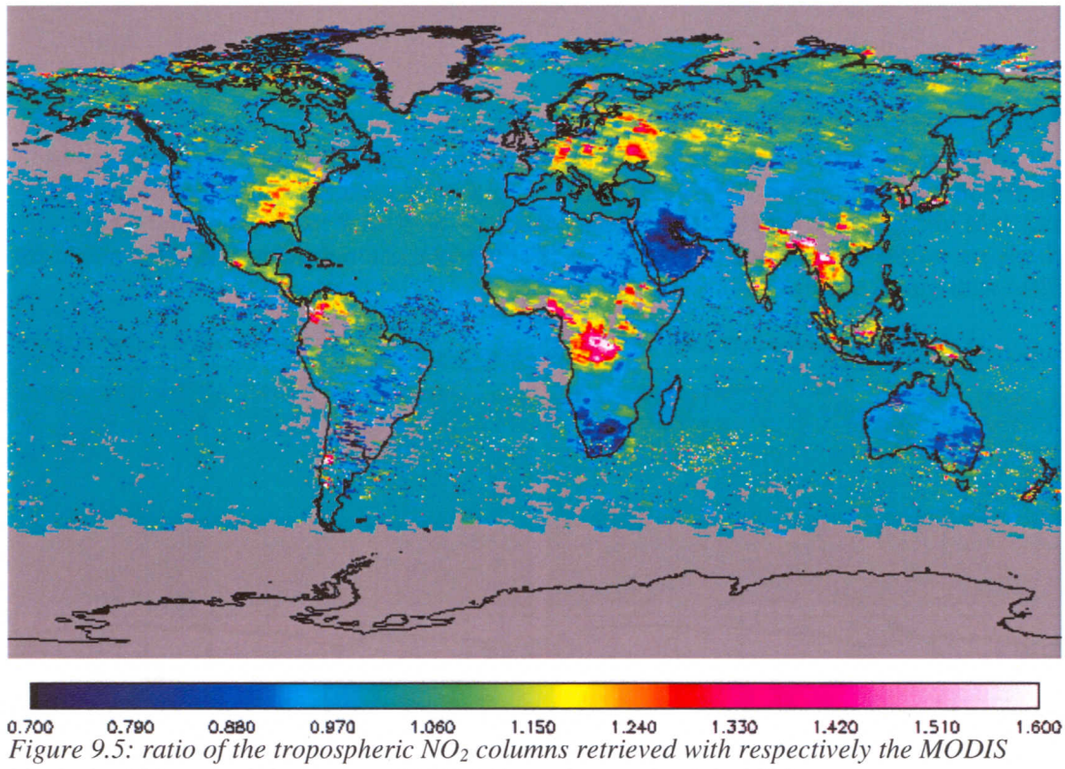

Figure 9.5: ratio of the tropospheric NO_2 columns retrieved with respectively the MODIS black-sky 460 nm and the current TOMS 440 nm dataset for July 1998

10 Conclusions and outlook

In the comparison of the albedo datasets derived from TOMS, GOME and MODIS, some differences arise.
It appears that on average the white-sky albedo has 7% percent higher values than the black sky albedo. The largest ratios are situated in areas with the lowest albedo values. Even there the absolute differences are small. It is known that the amount of direct illumination is about 80% for 440 nm. Therefore it is concluded that the true albedo, which is a linear combination of the black-sky and the white-sky albedo, can be approximated by the black-sky albedo.
The ratio of the GOME 440 nm dataset divided by the GOME 380 nm dataset is used to perform a spectral correction for the current TOMS 380 nm albedo dataset. It appears that the wavelength dependency of the albedo in that range is quite large. On average the GOME 440 nm albedo values are 60% higher than the GOME 380 nm values over land in the month of August.
From the comparison of the GOME 440 nm and the GOME 463 nm albedo dataset, it appears that the mean ratio of these datasets over land is about 0.97 for the month of August. Thus, on average the albedo values are 3% smaller at 440 nm than at 463 nm. However locally, over the rainforests, the albedo values are up to 10% larger at 440 nm. It is concluded that this wavelength difference has not a significant effect on the albedo values. Therefore, the MODIS albedo dataset at 459-479 nm can be used as a good approximation for the albedo at 440 nm, which wavelength is required in the NO_2 retrieval. A wavelength correction will locally give better results.
In the comparison of the current spectrally corrected TOMS albedo dataset and the GOME albedo dataset, it appears that these datasets match well on average, except for relatively low albedo values. Locally there is a large spread in values. For low albedo values GOME has slightly higher values at the northern hemisphere and slightly lower values in Southeast Asia, the west coast of Africa and parts of South America.
The spectrally corrected TOMS albedo dataset, and the MODIS black-sky albedo dataset appear to be very different. Large parts of North America, Europe and Asia have a 3 times lower albedo for MODIS with respect to TOMS. For the rainforests in South America, Central Africa and Southeast Asia this is even 3-5 times lower. Dry areas like desserts have a 2 times higher albedo for MODIS with respect to TOMS.
The NO_2 retrieval requires a reflectance, while for MODIS the black-sky albedo is used. The MODIS black-sky albedo appears to be an approximation of the MODIS surface reflectance for SCIAMACHY geometry. The ratio of them is on average 1.27. Because of the fact that the surface albedo can be considered as a mean reflectance and the geometries are quite similar, the black-sky albedo does not differ very much with the surface reflectance. In comparison with the large differences with the current TOMS albedo dataset, this difference of 27% is relatively small. It is concluded that the MODIS black-sky albedo can be used for investigating the effect on the NO_2 retrieval, but the resulting differences are an overestimate.

To test the impact of a different albedo dataset on tropospheric trace gas retrievals, the MODIS black-sky albedo dataset is used in the NO_2 retrieval for the month July 1998. The result is compared with the case that the current TOMS albedo dataset is used. Using the MODIS dataset results in about 20% higher NO_2 values in the heavily polluted areas as well as in the rainforest areas. In South Africa and Saudi Arabia the NO_2 concentrations are up to about 20% lower.

Over Northwest Europe a mean change of a factor 1.23 was expected. Over France this factor appeared to be 1, over The Netherlands 1.15 and over Germany 1.3. When the albedo values of these countries are examined, it appears that the albedo difference over France is less than the mean difference, while over Germany the albedo difference is larger. The difference over The Netherlands is almost the same as the average. It is concluded that on average this was a good estimate and that the same method of estimation can be used for other areas.

In this report only 1 month of albedo values is used in order to demonstrate the effect of using the MODIS albedo dataset. Other months showed mainly the same characteristics in the comparisons between the datasets.

The results of the study described in this report show that there are large differences between the MODIS dataset and the spectrally corrected TOMS dataset. The knowledge of the available albedo datasets and especially the MODIS BRDF/Albedo dataset has increased, but the differences in the albedo datasets are not fully understood yet. Because of the high resolution of MODIS, validation measurements can be performed easier and more accurate. The MODIS albedo values appear to correspond better to validation measurements, especially for low albedo values. In those regions it is known that TOMS and GOME give too high albedo values. A suggestion for the cause of this and other differences in the albedo datasets is that the TOMS and GOME albedo datasets are still contaminated with clouds and aerosols.

The effects of a different albedo dataset on the NO_2 retrieval are investigated and appeared to be very large. From these large differences, the high resolution of MODIS and the good correspondence of MODIS with validation measurements, it is recommended to do further research. The large differences between the albedo datasets need to be investigated further and need to be explained, before the MODIS dataset actually can be used in the NO_2 retrieval.

It is recommended to make a climatologic reflectance dataset for the retrieval geometry with the MODIS BRDF parameters. In the study described in this report this is only done without using quality information, which results in a map with cloud and snow contamination. In order to improve this, the quality factor provided in the MODIS dataset needs to be implemented in the determination of the reflectance values.

In the NO_2 retrieval an algorithm for cloud contamination is used, which is called FRESCO. This algorithm also uses an albedo dataset, but at wavelengths around 760 nm. MODIS has no albedo datasets at a wavelength close by. The nearest datasets are at 645 and 860 nm. In order to use the higher resolution MODIS dataset, it is necessary to investigate the wavelength dependency for every pixel. Then the albedo value for every pixel for a custom wavelength can be determined by interpolation. With some adjustments of the algorithm, this can make the NO_2 retrieval more accurate and less sensitive for cloud contamination.

Other ways that might give small improvements for the MODIS datasets are a wavelength correction, which locally might give better values, and a true albedo determination where needed.

The new NO_2 columns need to be validated. Then it can be checked whether the new results correspond better with the ground measurements. If this is the fact and the differences between the different datasets are explained, the replacement of the current albedo dataset by the MODIS dataset will certainly be a good improvement.

11 References

[1] K.F. Boersma et al, "Error analysis for tropospheric NO_2 retrieval from space", Journal of geophysical research vol. 109 D04311, 2004
[2] F. Gao et al, "Deriving albedo from coupled MERIS and MODIS surface products", Proc. MERIS Workshop, 2004
[3] F. Gao et al, "MODIS bidirectional reflectance distribution function and albedo Climate Modelling Grid products and the variability of albedo for major global vegetation types", Journal of geophysical research vol 110 D01104, 2005
[4] J.R. Herman et al, "Earth surface reflectivity climatology at 340-380 nm from TOMS data", Journal of geophysical research vol 102 D23 28003-28011, 1997
[5] R.B.A. Koelemeijer et al, "A database of spectral surface reflectivity in the range 335-772 nm derived from 5.5 years of GOME observations", Journal of geophysical research vol 108 D2 4070, 2003
[6] K.N. Liou, "An introduction to atmospheric radiation", International geophysics series volume 84, Academic Press, 2002
[7] R.D. McPeters et al, "Earth Probe Total Ozone Mapping Spectrometer (TOMS) Data products user's guide, NASA technical publication, 1998
[8] C.B. Schaaf et al, "First operational BRDF, albedo nadir reflectance products from MODIS", Remote sensing of environment 83 135-148, 2002
[9] A.H. Strahler et al, "MODIS BRDF/Albedo Product: Algorithm Theoretical Basis Document Version 5.0, NASA, 1999
[10] ftp://modis-atmos.gsfc.nasa.gov/L3LandSurfaceProducts/Data/Albedo/Maps/Product/, MODIS black-sky and white-sky albedo datasets at 1/60 degree in HDF format
[11] ftp://e0dps01u.ecs.nasa.gov/MOLT/MOD43C2.004/, MODIS BRDF parameters at 0.05 degree in HDF format, (all BRDF parameters files can be ordered through the DAAC Datapool or the EOS Data Gateway)